RADIANCE DISTRIBUTION AS A FUNCTION OF DEPTH IN AN UNDERWATER ENVIRONMENT

BY

JOHN E. TYLER

BULLETIN OF THE SCRIPPS INSTITUTION OF OCEANOGRAPHY
OF THE UNIVERSITY OF CALIFORNIA
LA JOLLA, CALIFORNIA

Volume 7, No. 5, pp. 363–412, plates 1–5, 2 figures in text

UNIVERSITY OF CALIFORNIA PRESS
BERKELEY AND LOS ANGELES
1960

CONTENTS

Abstract 363
Introduction 363
  Acknowledgments 364
Pertinent Description of Lake Pend Oreille 364
Description of Experimental Set-up 365
Instrumentation 365
Homogeneity of the Water 367
  Bathythermograph measurements 367
  Beam transmittance 367
  Particulate matter 367
Constancy of Surface Lighting 368
Plan of Operation 368
Discussion and Treatment of Data for Clear Sunny Conditions 369
  Calibration correction 371
  Changes in ambient light level 371
  Azimuth motion of the sun 371
  Barge image and shadows 371
  Graphical smoothing and interpolation of data 371
  Duplicate runs 372
  Depth-difference correction 372
  Sun altitude changes 372
  Normalization to the vertical run 372
Data for Clear Sunny Conditions 373
Discussion of Data and Evaluation of Sources of Error 373
Discussion and Treatment of Data for Overcast Conditions 381
Data for Overcast Conditions 381
Discussion of Data and Evaluation of Sources of Error 387
Asymptotic Radiance Distribution 387
Literature Cited 403
Plates 407

RADIANCE DISTRIBUTION AS A FUNCTION OF DEPTH IN AN UNDERWATER ENVIRONMENT

BY

JOHN E. TYLER

ABSTRACT

From the physical point of view the spatial distribution of radiance at various depths underwater provides by far the most useful description of the light field. From detailed radiance distribution data of this kind it is possible to obtain many of the important optical constants of the water and to make predictions regarding the penetration of light through water. For the purpose of checking theoretical relationships, and of designing and checking instrumentation, and for many other purposes, it is not important whether the water studied is fresh or salt, turbid or clear, since these parameters influence only the magnitudes of the quantities and constants involved.

In this investigation it was important that the water sample be deep and homogeneous throughout, and that the band width of radiation employed be narrow and consistent with depth. A detailed description of the experimental location establishes qualitatively or quantitatively the influence of various factors such as water depth, sky conditions, water surface conditions, water homogeneity, etc., on the data. Tables of radiance distribution data are given for seven depth stations under clear sunny conditions and for five depth stations under overcast conditions. The treatment of the original data to eliminate the effects of ambient light-level changes, changes in the position of the sun, etc., and to obtain tables based on a single sun altitude is discussed in detail.

The limiting shape of the radiance distribution, predicted by other workers and referred to here as the asymptotic radiance distribution, is discussed and tables of radiance K values are given. These latter data can be used to follow the changes in shape of the radiance distribution and to extrapolate these changes to even greater depths.

INTRODUCTION

DURING THE decade from 1935 to 1945 there seems to have been considerable interest in the angular distribution of natural light underwater. Ingenious measuring instruments were devised, including the "shadowing-screen" photometer described by Pettersson (1938) and also by Johnson and Liljequist (1938), and the Gershun tube photometer (Gershun, 1939) which directly limited the solid angle of acceptance. The objective of the work during that period seems to have been largely exploratory, although a theoretical treatment based on isotropic scattering was published by Poole (1945). Observations made on clear sunny days were compared with those on overcast days. Observations were also made at various depths and through various color filters. The light field was explored in a vertical plane in the sun's direction and in the vertical plane at right angles to the sun's direction. In addition, both Johnson and Liljequist (1938) and Whitney (1941*a*, *b*) explored the light field with azimuth sweeps taken at various angles from the zenith. It was observed that the angular distribution pattern of the natural light field changed in shape with depth, and it was surmised that at some unknown depth an equilibrium shape would be reached. It was also noted that the direction of the "bright" spot in the underwater light field tended to approach the zenith as depth was increased.

Although earlier data were adequate for the purpose for which they were intended, they do not now permit detailed investigations of the submarine light field or the computation of water constants. The resolving power of the instruments used was

never better than 15° (this refers to the apex angle of the circular cone of collection). Large solid angles of collection average too much information, especially in the direction of the sun, and tend to broaden the shape of the distribution diagram in that direction and at the same time tend to lower the apparent value of the peak radiance.

The data from the various publications cannot be combined to yield a single description of the light field because of differences in geographical location or instrumentation details (for example in the selection of filters and photo cells). The papers individually have insufficient information on the homogeneity of the water sample that was being measured, and, for computational purposes, have insufficient data points covering the radiance of the submarine light field.

The importance of the radiance distribution of the natural underwater light field as a primary means for documenting the optical properties of large bodies of water was first recognized by S. Q. Duntley in 1949 while he was conducting research on visibility problems in scattering-absorbing media. At that time Dr. Duntley initiated a program of instrument development and study which has been continued to the present time.

Some of the theoretical work accomplished by this program has been published by Duntley (1952) and Preisendorfer (1957*a*) and some is being brought to the attention of the Optical Society of America by Preisendorfer (1958*b*, *c*). The development of instrumentation for the detailed measurement of radiance distribution was first described by Duntley *et al.* (1955) and the program of work in progress at that time was discussed by Tyler (1955). Following the summer of 1956, major design changes were made in the instrumentation and in the spring of 1957 field operations were conducted in deep water at the United States Navy Electronics Laboratory Calibration Station on Lake Pend Oreille in northern Idaho.

The objective of the 1957 field work was to obtain detailed data on radiance distribution as a function of depth in homogeneous water under "clear sunny sky" and "overcast sky" lighting conditions. Since the work was expected to provide new data with which to test the theory of radiative transfer through a hydrosol, measurements were confined within a narrow wavelength band.

ACKNOWLEDGMENTS

I wish to acknowledge the inspiration and guidance of S. Q. Duntley whose long-term interest in the optics of scattering-absorbing media has been the motivating force behind this investigation. I also wish to acknowledge the work of R. W. Austin and associates in the design, construction, and testing of the underwater photometer, of R. W. Holmes who took part in the examination of the lake water for homogeneity, and of W. H. Richardson who assisted in the data reduction.

This paper, in part, represents results of research supported by the U.S. Navy Bureau of Aeronautics and the U.S. Navy Bureau of Ships and carried out by the University of California under a Bureau of Ships contract.

PERTINENT DESCRIPTION OF LAKE PEND OREILLE

Lake Pend Oreille is in many ways ideally situated for underwater optical investigations. The field station is a barge moored at the south end of the lake about 2 miles from the village of Bayview and about half a mile from the nearest shore line.

Cape Horn Peak to the north rises 16.5° above the horizon, and peaks of the western edge of the Bitterroot Mountains block out, at most, 12.5° of the sky to the south. To the east and west the sky line is much lower than this. Although the effect of the sky line on the submarine light field is not yet known, it is presumed to be small owing to Fresnel reflection at these high angles of incidence, and also owing to the fact that refraction reduces the angular subtense of the sky line so that the 16.5° between sky line and horizontal becomes only 2.7° in the underwater scene.

The major inlet of Lake Pend Oreille is Clark Fork some 20 miles to the north of the station and practically in line with the Pend Oreille River, which is the major outlet. Thus the largest source of particulate matter has little effect on the water near the station. The eleven streams and creeks along the south and east shore line which were examined at the time of the experiment were all carrying clear water from melting snow over streambeds of clean boulders.

The lack of major currents in the lake, the somewhat stagnant location of the station, and the absence of silt-laden drainage into the southern end of the lake all helped to minimize the possibility of stratification or inhomogeneity in the water.

DESCRIPTION OF EXPERIMENTAL SET-UP

The Pend Oreille Calibration Station is a two-story, 40- by 40-foot barge floated on T6 pontoons and held in place by mooring cables designed to minimize yaw. The siding, at the time of the experiment, was painted light green and as a result, the barge, at noon, exhibited high positive contrast as seen from the instrument. The new underwater photometer was suspended from a single supporting cable at the end of a 30-foot boom on the south side of the building. The inboard end of the boom was fastened to the barge near the water line and the outboard end was about 6 to 8 feet above the water. The instrument was thus 30 feet or more from the barge at all times. The maximum horizontal angles subtended by the barge at the point of immersion were 45.5° to the east, 8.5° to the west, and about 33.7° in the vertical direction. From a point below the surface the barge subtended a vertical angle of about 10° at the instrument, and appears in the data between tilt angles of 38° and 48°. The image of the barge and the submarine shadow created by the barge have a noticeable effect on the natural-light field near the surface and a detectable effect even at the deeper stations. The depth of water below the station is 750 feet which assured the absence of bottom reflectance effects in the measurements.

INSTRUMENTATION

All of the radiance distribution data presented herein were taken with the underwater photometer shown in plates 1 and 2. This instrument was suspended on a single cable and powered by a 31-conductor electric cable looped into the underside at the vertical axis of rotation as shown in plate 3. The instrument was thus free to rotate around a vertical axis. Rotation about this axis was controlled by means of a gyrosyn compass assembly in the azimuth-position control box with input control and gyro repeater on the main control panel. The error signal resulting from an azimuth mismatch between the control transformer and the gyro heading was used to drive a propeller that rotated so as to minimize the error signal. With this mechanism it was possible to maintain an azimuth setting of $\pm 1°$ or better. For all the data presented here the azimuth error is less than $\pm 1°$.

TABLE 1

MEASURED TRANSMITTANCE OF WRATTEN NO. 45 GELATINE FILTER

λ (mμ)	T (%)	λ (mμ)	T (%)	λ (mμ)	T (%)	λ (mμ)	T (%)
203	0.0	433	1.0	40	0.0	70	89.8
10	0.0	40	3.4	50	0.0	80	89.5
20	0.0	50	10.0	60	0.0	90	89.8
40	0.0	60	15.0	70	0.0	900	89.8
50	0.0	70	17.0	80	0.0	10	89.8
60	0.0	80	17.6	90	0.0	20	89.8
70	0.0	490	16.9	700	0.3	30	89.8
80	0.0	500	14.4	10	3.3	40	89.8
90	0.0	10	10.0	20	19.0	50	89.8
300	0.0	20	5.3	30	42.5	60	89.5
10	0.0	30	2.0	40	62.0	70	89.8
20	0.0	536	1.0	50	74.5	80	89.8
30	0.0	40	0.3	60	80.8	90	90.0
40	0.0	546	0.1	770	84.0	1000	90.2
50	0.0	50	0.0	80	86.0	1100	90.8
60	0.0	60	0.0	90	87.0	1200	90.5
70	0.0	70	0.0	800	87.5	1300	86.5
80	0.0	80	0.0	10	87.8	1400	76.5
90	0.0	90	0.0	20	88.5	1500	56.5
400	0.0	600	0.0	30	88.8	1600	44.5
10	0.0	10	0.0	40	89.0	1700	35.0
20	0.0	20	0.0	50	89.5	1800	27.0
30	0.1	30	0.0	60	89.6	1900	22.0

The optical system of the underwater-photometer measuring head, shown in plate 4, is a dual detecting system, each channel consisting of a 931A multiplier phototube wrapped with black tape except for a window covered with a Wratten No. 45 blue-green gelatine filter. The measured transmittance characteristics of this filter are shown in table 1. Since the readings obtained are proportional to

$$\int_{\lambda_1}^{\lambda_2} EST_F\, T_W\, d\lambda$$

E = Energy distribution of the light just below the surface
S = Spectral sensitivity of phototube
T_F = Transmittance of No. 45 filter
T_W = Transmittance of water path
λ = Wave length of light

and since the combination ST_W establishes the value of the limiting wave length λ_2 at about 700 mμ or less, it can be seen that these data are tagged with an energy distribution having half-band width of 64mμ and extreme limits between 430 mμ and 546 mμ. Deep-water measurements in this region of the spectrum would not necessarily require an auxiliary filter since the combination of water and phototube sensitivity would provide all the "filtering" action required. In this work the

Wratten No. 45 filter was used simply to make the shallow-water measurement consistent in band width with the deep-water measurements.

In order to extend the range of measurement, each multiplier phototube is surrounded by a cylinder containing openings covered by filters having neutral densities of about 0, 1, 2, 3, 4, and infinity. The window in the pressure housing is frosted on the inside to assure a constant coupling factor between the collecting system and the multiplier phototube. The internally baffled radiance tubes limit the angle of acceptance to 6.6°. The whole head can be tilted through a range of somewhat more than 180° by means of a synchronous motor. Event marks are automatically recorded at a specific angle at the beginning of the tilt sweep.

HOMOGENEITY OF THE WATER

Considering the intended application of these data, namely, to examine the ability of current theory to describe and predict the passage of natural light through a homogeneous hydrosol, it was of the utmost importance for the water sample to be homogeneous. The favorable location of the barge and the absence of conditions likely to produce inhomogeneity in the water have already been mentioned. The water itself was also examined for evidence of inhomogeneity. This examination consisted of the following tests:

A. Bathythermograph measurements. It is well known that certain lakes, including Lake Pend Oreille, undergo seasonal changes in their temperature profile, that warm weather will develop a layer of warm water at the surface and various kinds of microörganisms will "bloom" in or near this warm layer. Stratification of this type means discontinuous changes in the structure of the light field as a function of depth, a condition that would not yield suitable data. The absence of a thermocline implies that the bloom has not occurred and that this source of inhomogeneity is absent.

Bathythermograph measurements were made at frequent intervals during the entire operation and consistently showed no thermocline. The record for 16 March, for example, shows a surface temperature of 2.35° C rising at constant rate to 3.20° C at 122 m depth. The record for 29 April shows a constant temperature of 3.6° C from the surface to 137 m. More critical examination (on 29 April 1957) of the top 2 m with a bucket thermometer showed 4.5° C at the surface, 4.0° C at 1.25 m and 4.0° below 1.25 m, indicating a calibration error in the bathythermograph that is not significant to these light measurements, and possibly a slight surface heating owing to full sunshine on 28 April. All other bathythermograph records were, happily, monotonously the same.

B. Beam transmittance. Beam transmittance and its variability with depth were measured with a beam transmissometer. Total transmittance for a collimated beam of light was 67.3 per cent per meter at the surface and increased at a steady rate to about 68.6 per cent per meter at 61 m (measurements of 29 April 1957). Other determinations taken during the period of field operations showed no significant variation from this condition.

C. Particulate matter. One- and two-liter samples were taken with a Nansen bottle at discrete depths from 6 m to 60 m and filtered through Millipore H A filters having a pore size of 0.45μ ($\pm$) 0.02μ. Results are shown in table 2.

Although each of the above tests seems to exhibit a trend with increasing depth the

trends are conflicting and the variations of the parameter in each instance is close to the expected error. Definitive evidence of stratification or inhomogeneity was considered to be absent during the period of the experiment.

Further evidence of the homogeneity of the lake water is provided by the results of calculations from radiance distribution measurements.

TABLE 2

WEIGHT OF PARTICULATE MATTER FOUND IN WATER SAMPLES TAKEN FROM THE DEPTHS SHOWN

Depth (meters)	Particulate matter (mg per liter)
6.1	0.32±.07
12.2	0.37
24.4	0.40
30.5	0.41
48.8	0.51
54.9	0.41
61.0	0.55

CONSTANCY OF SURFACE LIGHTING

The natural lighting on the surface of the water can undergo changes in ambient level and also in structure, that is, in the position of bright spots, such as the sun or single white clouds, or in the relative proportions of specular to diffuse light. The effect of very slow changes in ambient level can be successfully corrected but no method is known at present which will properly correct for the effect of rapid changes in ambient level or for the effect of changes in the structure of the light field. One must wait for desirable lighting conditions and even then may be forced to reject some data because of these uncontrollable variables.

For several years now it has been the practice in this laboratory to monitor the natural lighting at the surface with an instrument sensitive to both the light level and to its structure, and, on the basis of this record, to sort and reject data. For the data taken on 28 April no rejection was indicated.

PLAN OF OPERATION

The plan of operation was dictated to a large extent by azimuth and elevation changes in the sun's position, by the proposed computations from the data, and by the operating characteristics of the instrument. For computational purposes, data were needed at equally spaced azimuth intervals. A 20°-azimuth interval would give eighteen continuous tilt sweeps with each measuring channel, or two complete radiance distributions at a fixed depth station in 25 minutes. In the progress of such a run a sweep by one radiance tube would be repeated 12.5 minutes later by the sweep of the opposite radiance tube.

The most favorable period for making the measurements would be within two hours each side of noon (sun time) since this is the period of minimum change in sun elevation and consequently of minimum change in ambient light level and structure. Allowing 30 minutes at each station would provide for eight stations

between 1000 and 1400. Some ambient light-level changes would, of course, occur during this 4-hour period because of changes in the position of the sun. In order to obtain data on the zenith and nadir radiance for different depths which would be independent of ambient light-level changes, a monitoring run was planned for noon. For this run the radiance tubes were set in a vertical position and measurements were made at discrete depths, including all station depths, in about 10 minutes. Thus in the final data reduction all radiance distributions for the day could be adjusted to a single sun altitude.

DISCUSSION AND TREATMENT OF DATA FOR CLEAR SUNNY CONDITIONS

Data recording on 28 April was begun at 0850 at a depth of 66.1 m and continued until 1441. The order of depth stations is important because the structure of the light field is a function of depth as well as sun position. The order used is given in table 3.

TABLE 3

ORDER OF DEPTH STATIONS FOR 28 APRIL 1957

(All times are Pacific Standard; sun noon occurred at very nearly 1140 P.S.T.)

Depth (meters)	Time (P.S.T.)		Elapsed time (minutes)	Sun altitude (degrees)		Sun azimuth (degrees)	
	Start	Stop		Start	Stop	Start	Stop
66.1	0852	0924	32	41.0	45.5	119.0	127.5
53.7	0927	0947	20	46.0	48.5	128.0	134.0
41.3	0949	1009	20	48.5	51.0	135.0	142.0
29.0	1012	1033	21	51.0	53.0	143.0	150.5
16.6	1039	1103	24	53.5	55.0	153.0	162.5
10.4	1105	1126	21	55.0	55.5	163.5	172.5
4.2	1128	1152	24	55.5	55.5	173.5	183.5
Vertical run	1158	1210	12	.2 change		186.0	191.5
66.1	1211	1249	38	55.5	53.5	192.0	207.5
53.7	1252	1313	21	53.0	51.5	208.5	216.0
41.3	1316	1338	22	51.0	48.5	217.0	224.5
29.0	1341	1402	21	48.5	45.5	225.5	232.0
16.6	1405	1425	20	45.0	42.5	233.0	238.5
Vertical run	1432	1441	9	1.2 change		241.0	243.0

The original data clearly show the features of the environment. The image of the sunlit barge wall is obvious at the shallow stations and the shadow of the barge can be seen at all stations although it is not obvious at the deeper ones (see fig. 1). The position of the "bright spot" is always recognizable and at the shallow stations the edge of the "man hole" can be seen, as can the shadow of the instrument itself. In addition, changes in the sun's azimuth position and in its elevation can be detected in the data.

In order to remove the effect of these unwanted parameters from the data the following procedural steps were adopted:

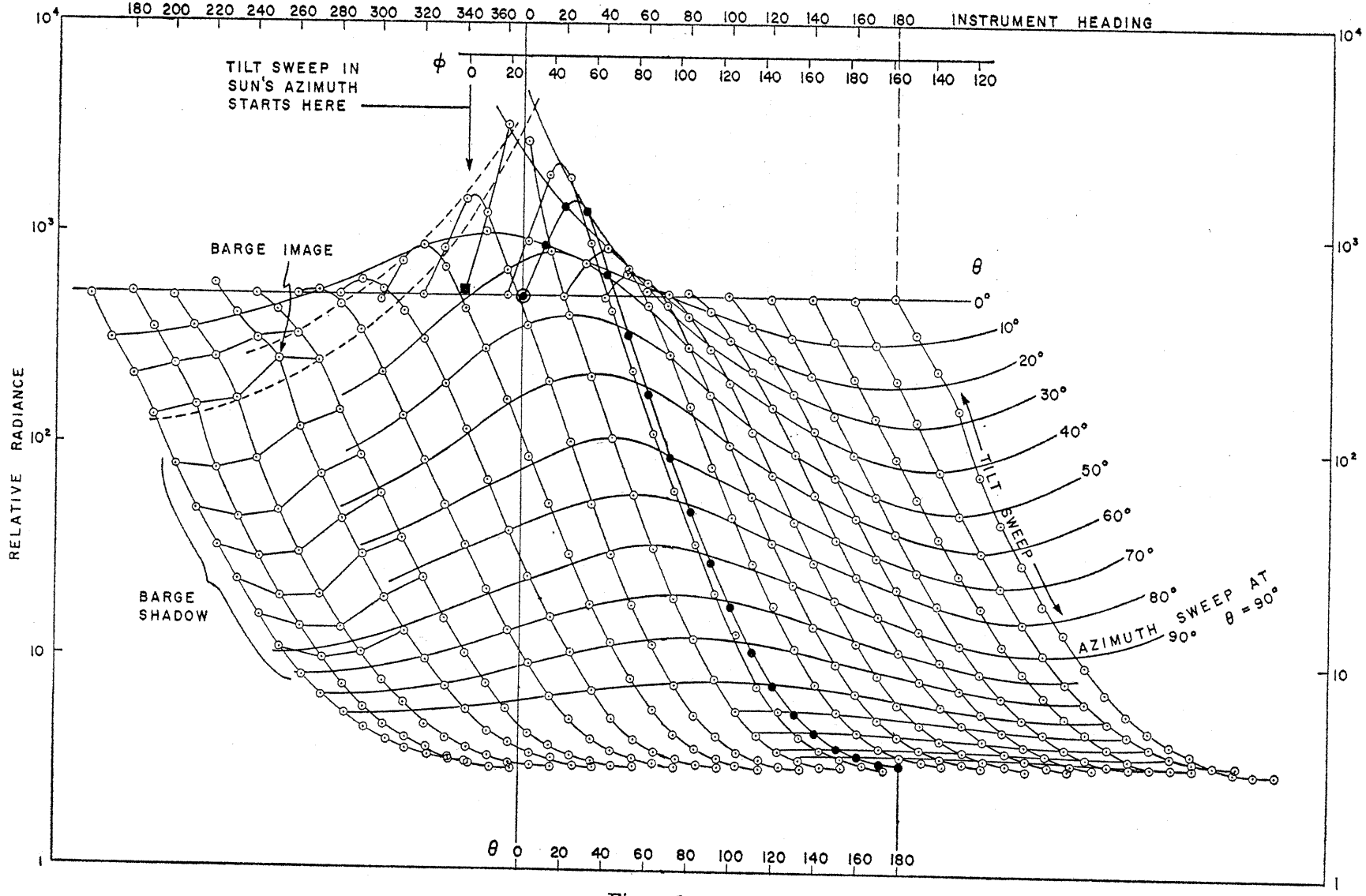
INSTRUMENT HEADING
TILT SWEEP IN SUN'S AZIMUTH STARTS HERE
BARGE IMAGE
BARGE SHADOW
RELATIVE RADIANCE
TILT SWEEP
AZIMUTH SWEEP AT θ = 90°

Figure 1

1. *Calibration correction.*—The original data, which are very nearly linearly proportional to the log of the radiance, were read at 10-degree intervals of tilt with a special "rule" which converted the data to radiance units and at the same time removed the small departures from linearity that were known to be present. Each information channel, consisting of the multiplier phototube, the chassis and the recorder, has its own calibration "rule." The data for these rules were obtained at the site of the experiment just before and just after the measurements.

2. *Changes in ambient light levels.*—Inspection of the data for the nadir direction indicated the extent of the ambient light-level change owing to changes in the position of the sun. When necessary this has been corrected by normalizing all tilt sweeps for the station to the average nadir reading.

3. *Azimuth motion of the sun.*—The data thus obtained were replotted on semi-log paper, as shown in figure 1. The known azimuth angle between the sun and the instrument heading has been used to locate each tilt sweep on the plot. Thus the azimuth motion of the sun relative to the instrument is not superimposed on the data. (For a complete explanation of figure 1, see step 5.)

4. *Barge image and shadows.*—The data points resulting from step 3 were joined by smooth curves to give azimuth sweeps at constant tilt as well as tilt sweeps at constant azimuth (see fig. 1). The image of the barge, its shadow, etc., can be positively identified in these plots. Sections of the data which were distorted by these spurious signals were not used in the data reduction. The physical location of the instrument was such that a maximum of only about 54° of the horizontal sweep was distorted by the presence of the barge. Data on the left of the sun's plane in figure 1 could be checked by superposing the data on the right of the sun's plane. The position of the sun was located by the maxima of the azimuth sweeps and checked with the known position of the sun in each instance.

5. *Graphical smoothing and interpolation of data.*—In figure 1 the values of the angles at the top, marked "instrument heading," are relative to a fixed compass direction. These angular values are related to the actual angle between the sun and the "instrument heading" through elapsed time. In the depth station illustrated the instrument was rotating "with the sun" and the actual angle was always less than the indicated angle by the amount of angular change in the sun's position during the time interval between the beginning of one tilt sweep and the next. As an example, in the time it took to complete a sequence of tilt sweeps from an indicated instrument heading of 0° to one of 360° the sun's position had changed 8°. Actual rotation of the instrument from the sun was therefore 352°. Thus in the plot the "instrument heading" of 360° is plotted at 352° along the abscissa. The marks on the "instrument heading" scale therefore represent the actual angle between the instrument heading and the sun. Each mark coincides with the first datum point of a tilt sweep. The instrument heading of 0° coincides with the tilt sweep whose first datum point is double circled in figure 1. The data points on this particular tilt sweep (solid circles) are identified with the scale of tilt angles θ at the bottom of figure 1.

Each of the twenty-one tilt sweeps included in figure 1 will have a datum point at $\theta = 90°$ (for example). The procedure that has been used to plot the twenty-one tilt sweeps has placed the $\theta = 90°$ points in proper relation to one another so that a line joining them graphically represents an azimuth sweep at $\theta = 90°$. The other

points of the figure have been similarly joined permitting a sort of two-dimensional smoothing of all the data at once.

During the experiment it was not practical to orient the instrument heading with the sun's position. Thus in the working plots the sun's position, which is indicated by the maxima of the azimuth sweeps, bears no relationship with the "instrument heading" scale at the top. The scale marked ϕ (also at the top) has been drawn so that $\phi = 0°$ is in the sun's direction for the azimuth sweep marked $\theta = 0°$ (a straight line). (In figure 1 the sun's direction, for the $\theta = 0°$ curve only, solid square, happens to coincide very nearly with the 340° instrument heading.)

In order to obtain radiance data at equal intervals on each side of the sun's position and for all tilt angles, the ϕ scale is moved right 10° for each successive azimuth sweep. For each such setting the desired data can be interpolated from the azimuth curves.

6. *Duplicate runs.*—Both information channels functioned perfectly during the entire experiment and consequently duplicate runs were available at all depth stations. These were treated independently through step 5, above, and the interpolations were then averaged. A double run was made at the 66.1-m station giving a total of four complete determinations at this depth. All four determinations are averaged together in this instance.

7. *Depth-difference correction.*—The ends of the brightness tubes are about 0.5 m from the center of rotation of the measuring head. As a result the station depth does not remain quite constant but changes continuously with tilt angle according to the equation

$$Z_t = Z \pm r \cos \theta .$$

Where Z_t is the true depth, Z is the reported station depth to the center of rotation of the instrument and r is the distance from the center of rotation to the end of the radiance tube.

The averaged data from step 6 were corrected to give the radiance distribution at a point by determining the slope of the curve of path radiance vs. depth for every pair of values of tilt angle and azimuth angle and making the proper correction along this slope.

8. *Sun altitude changes.*—In addition to changes in ambient light level at the surface of the water, large changes in the altitude of the sun result in a change in the ratio of the zenith to nadir path radiance and a reorientation of the whole radiance distribution solid in the direction of the sun. The depth stations were taken in the order shown in table 3 so that the shallow stations should be at noon and the others clustered around noon in such a way that a complete set of stations could be slected from those nearest noon. Changes in the shape of the distribution solid owing to changes in the sun's altitude were this way minimized.

9. *Normalization to the vertical run.*—Before the seven morning runs could be normalized to the single vertical run at noon it was necessary to demonstrate that the radiance distribution solid for the 66.1-m station was substantially the same in shape at 0908 as it would have been at 1200, that the radiance distribution solid for the 53.7-m station was substantially the same in shape at 0937 as it would have been at 1200, and so on. To do this the ratio of the average zenith to average nadir reading for each depth station was compared with the ratio of the zenith to nadir

reading found from the noon vertical run. For all depth stations, duplicate ratios were found, indicating that no significant error is introduced by adjusting these runs to a single sun altitude. It was also found that the complete data for the 66.1-m and 53.7-m morning stations duplicated the data for the 66.1-m and 53.7-m afternoon stations. Since the former were completed two hours before sun noon and the latter were obtained within about two hours after sun noon, this is further evidence that changes in sun elevation did not significantly affect the shape of the distribution solid at the deep stations. For the remaining morning stations the change in sun altitude between station time and 1200 is very small indeed. After refraction the change in sun angle from 1000 to 1200 is only four-tenths of the resolving power of the radiance tube. It is progressively true throughout the morning data that the large incremental changes in the sun's altitude coincide with the depth stations where such changes have the least effect on the shape of the distribution solid, and the near-zero changes in sun's altitude coincide with the near-surface data where large changes would have had a very large effect.

On the strength of the above evidence, the data for the seven stations given in tables 4, 5, 6, 7, 8, 9, and 10 are presented as data for one sun altitude.

DATA FOR CLEAR SUNNY CONDITIONS

Data representing clear sunny conditions were obtained on 28 April 1957. The voice-recorded notes for the day read as follows:

> 28 April 1957. It would not be possible to have a more perfect day for the sunny-sky case than today. Between seven in the morning and three-thirty in the afternoon there were no overhead clouds whatsoever. The few small clouds that did appear just over the mountain peaks rapidly evaporated. At no time was it possible to see evidence of a high altitude cirrus layer. In addition to this the lake was practically flat calm all day.

Later computations placed the clouds mentioned at an altitude of 13° in the southern sky. They appeared one at a time and evaporated within 10 minutes. Their angular subtense was never more than 1.5°. The optical state of the lake surface is shown in the photograph, plate 5, taken on 28 April at about 1500.

The radiance distribution data for a clear sunny sky are given for seven depth stations in tables 4 through 10, inclusive.

DISCUSSION OF DATA AND EVALUATION OF SOURCES OF ERROR

In the body of tables 4 through 10 the over-all variation in the value of radiance at any one setting is ±5 per cent of the radiance at that setting. This variation includes instrument errors, reading and plotting errors, errors made in setting and holding azimuth positions during the experiment, and in fact all errors that have entered the measurements before their presentation in the tables.

In the direction of the sun, experimental azimuth steps of 20° move the acceptance cone of the instrument a distance that is almost equal to the base diameter of the acceptance cone. If the air-water boundary were flat the sun's image would therefore be within the cone only once during a complete set of azimuth settings. However, the direction of the sun is a glitter pattern whose size depends on the optical state of the surface (which in turn depends on the wind velocity). During the measurements of 28 April the wind velocity was less than 1 m per second which would indicate a glitter pattern considerably smaller than 10° in angular subtense

TABLE 4

RADIANCE DISTRIBUTION UNDER CLEAR SUNNY SKY
(Depth, 4.24 meters; Sun altitude, 56.6°)

Tilt angle (Θ)	Azimuth angle (Φ)									
	0	20	40	60	80	100	120	140	160	180
0	204,000	204,000	204,000	204,000	204,000	204,000	204,000	204,000	204,000	204,000
10	541,000	481,000	374,000	286,000	220,000	174,000	139,000	119,000	108,000	104,000
20	4,300,000	1,320,000	545,000	277,000	168,000	118,000	93,000	79,600	72,100	69,100
30	7,980,000	1,100,000	401,000	198,000	123,000	87,200	69,400	59,700	54,500	52,400
40	573,000	427,000	234,000	135,000	90,500	68,300	56,300	48,700	44,100	42,300
50	207,000	164,000	106,000	69,500	49,300	37,700	31,000	26,500	23,800	23,200
60	114,000	91,800	66,400	47,700	35,300	27,300	22,300	19,000	17,100	16,600
70	61,300	55,800	45,100	34,300	26,700	21,200	17,500	14,800	13,200	12,400
80	41,500	38,200	31,500	25,100	20,100	16,100	12,900	11,300	10,000	9,460
90	26,900	25,300	21,500	17,600	14,200	11,700	9,840	8,560	7,820	7,480
100	17,000	16,000	13,900	11,700	9,940	8,590	7,620	6,860	6,390	6,140
110	11,200	10,700	9,280	8,060	7,180	6,490	5,990	5,600	5,340	5,220
120	7,430	7,170	6,630	6,020	5,590	5,250	5,000	4,800	4,670	4,590
130	5,360	5,220	4,950	4,710	4,520	4,320	4,180	4,040	4,010	3,990
140	4,230	4,170	4,040	3,960	3,850	3,780	3,710	3,650	3,620	3,600
150	3,570	3,560	3,520	3,480	3,440	3,380	3,340	3,300	3,280	3,260
160	3,250	3,250	3,250	3,250	3,250	3,240	3,240	3,240	3,230	3,230
170	3,110	3,110	3,110	3,110	3,110	3,110	3,110	3,110	3,110	3,110
180	3,050	3,050	3,050	3,050	3,050	3,050	3,050	3,050	3,050	3,050

TABLE 5

RADIANCE DISTRIBUTION UNDER CLEAR SUNNY SKY

(Depth, 10.4 meters; sun altitude, 56.6°)

Tilt angle (Θ)	Azimuth angle (Φ)									
	0	20	40	60	80	100	120	140	160	180
0	127,000	127,000	127,000	127,000	127,000	127,000	127,000	127,000	127,000	127,000
10	274,000	258,000	215,000	166,000	129,000	103,000	86,800	78,300	73,300	71,400
20	1,970,000	610,000	284,000	158,000	101,000	72,000	57,300	49,600	46,500	45,400
30	2,540,000	472,000	208,000	110,000	68,500	49,200	39,000	33,400	30,900	30,300
40	298,000	207,000	118,000	71,000	46,900	34,400	27,200	22,900	20,300	19,200
50	118,000	104,000	69,900	45,900	31,300	23,000	17,700	14,800	13,500	13,000
60	55,900	51,400	41,000	29,400	20,400	14,700	11,600	9,670	8,700	8,360
70	32,500	30,100	24,000	17,900	13,200	10,100	8,150	6,800	6,100	5,860
80	18,100	17,200	14,700	11,400	8,740	6,900	5,660	4,800	4,320	4,150
90	10,600	10,100	8,700	7,020	5,630	4,640	3,960	3,530	3,320	3,270
100	6,500	6,160	5,540	4,800	4,000	3,380	3,000	2,730	2,590	2,540
110	4,320	4,120	3,750	3,320	2,880	2,500	2,260	2,110	2,030	2,010
120	2,940	2,830	2,640	2,440	2,220	1,970	1,840	1,750	1,700	1,690
130	2,020	1,980	1,930	1,860	1,770	1,720	1,630	1,570	1,540	1,530
140	1,630	1,620	1,610	1,570	1,540	1,500	1,450	1,420	1,390	1,390
150	1,410	1,410	1,400	1,370	1,350	1,330	1,310	1,280	1,260	1,260
160	1,240	1,240	1,240	1,240	1,240	1,240	1,240	1,240	1,230	1,230
170	1,180	1,180	1,180	1,180	1,180	1,180	1,180	1,180	1,180	1,180
180	1,180	1,180	1,180	1,180	1,180	1,180	1,180	1,180	1,180	1,180

TABLE 6

RADIANCE DISTRIBUTION UNDER CLEAR SUNNY SKY

(Depth, 16.6 meters; sun altitude, 56.6°)

Tilt angle (Θ)	Azimuth angle (Φ)									
	0	20	40	60	80	100	120	140	160	180
0	59,100	59,100	59,100	59,100	59,100	59,100	59,100	59,100	59,100	59,100
10	121,000	111,000	93,100	74,100	59,900	48,700	41,000	36,500	34,000	33,200
20	350,000	183,000	109,000	71,500	49,400	36,900	29,100	24,400	21,900	21,200
30	385,000	169,000	86,200	53,000	36,300	26,700	20,400	16,700	14,600	13,800
40	88,200	75,900	53,500	35,700	24,500	17,900	13,600	10,300	9,380	8,780
50	45,300	41,000	31,700	21,700	14,900	11,100	8,550	6,860	5,880	5,490
60	24,400	22,500	17,400	12,500	9,030	6,950	5,500	4,590	3,960	3,670
70	12,400	11,200	9,100	7,230	5,670	4,520	3,460	3,040	2,670	2,530
80	6,750	6,360	5,490	4,510	3,640	2,990	2,500	2,130	1,870	1,750
90	4,050	3,770	3,280	2,790	2,340	1,970	1,660	1,440	1,310	1,250
100	2,360	2,280	2,070	1,800	1,540	1,330	1,180	1,070	990	964
110	1,520	1,470	1,350	1,210	1,090	982	891	832	796	778
120	1,010	995	946	884	816	758	711	684	666	656
130	740	732	717	685	658	633	606	584	572	564
140	595	587	581	566	550	536	522	512	510	510
150	502	499	497	495	486	480	472	465	462	462
160	451	451	451	450	447	443	439	434	433	433
170	422	422	422	422	422	422	422	422	422	422
180	418	418	418	418	418	418	418	418	418	418

TABLE 7

RADIANCE DISTRIBUTION UNDER CLEAR SUNNY SKY

(Depth, 29.0 meters; sun altitude, 56.6°)

Tilt angle (Θ)	Azimuth angle (Φ)									
	0	20	40	60	80	100	120	140	160	180
0	9,630	9,630	9,630	9,630	9,630	9,630	9,630	9,630	9,630	9,630
10	14,300	13,300	12,000	10,600	9,460	8,410	7,540	6,850	6,330	6,080
20	22,100	16,300	12,100	9,530	7,730	6,440	5,490	4,750	4,220	3,980
30	20,000	13,500	9,280	6,990	5,560	4,620	3,900	3,320	2,880	2,680
40	9,970	8,090	6,080	4,740	3,820	3,110	2,590	2,180	1,820	1,660
50	5,110	4,610	3,750	3,040	2,490	2,030	1,650	1,350	1,100	993
60	2,780	2,490	2,070	1,730	1,440	1,210	1,010	842	708	651
70	1,440	1,330	1,140	986	839	719	618	530	455	425
80	799	739	657	579	505	444	389	343	303	281
90	470	447	412	365	323	287	254	225	202	191
100	293	278	256	231	210	192	175	159	148	143
110	191	185	172	159	150	138	129	121	113	111
120	135	130	123	116	110	105	98.9	94.2	90.0	88.6
130	99.2	97.0	93.6	90.1	87.3	84.1	80.5	78.3	76.4	75.5
140	79.6	78.4	76.4	74.6	73.4	72.1	70.5	69.1	67.8	66.5
150	68.3	67.6	66.3	65.8	64.7	63.7	62.8	61.8	61.3	60.6
160	60.4	59.9	59.6	59.1	58.9	58.5	58.1	58.0	57.4	57.3
170	56.2	56.2	56.2	56.2	56.2	56.2	56.2	56.2	56.2	56.2
180	55.2	55.2	55.2	55.2	55.2	55.2	55.2	55.2	55.2	55.2

TABLE 8

RADIANCE DISTRIBUTION UNDER CLEAR SUNNY SKY

(Depth, 41.3 meters; sun altitude, 56.6°)

Tilt angle (Θ)	Azimuth angle (Φ)									
	0	20	40	60	80	100	120	140	160	180
0	1,380	1,380	1,380	1,380	1,380	1,380	1,380	1,380	1,380	1,380
10	1,650	1,600	1,510	1,410	1,320	1,250	1,180	1,120	1,070	1,050
20	1,680	1,580	1,420	1,270	1,120	1,010	910	822	750	721
30	1,260	1,180	1,049	921	811	716	631	557	496	474
40	859	800	700	614	533	465	408	361	322	306
50	510	478	426	376	333	294	259	229	202	191
60	300	285	254	222	194	170	149	132	117	111
70	165	156	143	126	113	101	90.2	80.6	73.2	70.8
80	88.9	84.9	79.1	72.5	66.6	60.8	55.7	50.9	47.3	45.2
90	51.3	50.4	47.7	44.9	41.7	38.6	36.0	33.4	31.4	30.4
100	33.5	32.5	30.7	28.9	27.2	25.6	24.1	22.8	21.7	20.9
110	21.8	21.5	20.9	19.9	19.0	18.1	17.4	16.7	16.0	15.7
120	15.8	15.8	15.4	14.9	14.3	13.8	13.3	12.9	12.5	12.3
130	12.3	12.2	12.0	11.7	11.5	11.2	11.0	10.8	10.6	10.5
140	10.2	10.1	10.0	9.90	9.78	9.65	9.57	9.45	9.33	9.02
150	8.75	8.73	8.66	8.63	8.57	8.53	8.46	8.40	8.35	8.34
160	7.88	7.88	7.88	7.88	7.87	7.87	7.87	7.87	7.86	7.86
170	7.53	7.53	7.53	7.53	7.53	7.53	7.53	7.53	7.53	7.53
180	7.43	7.43	7.43	7.43	7.43	7.43	7.43	7.43	7.43	7.43

TABLE 9

RADIANCE DISTRIBUTION UNDER CLEAR SUNNY SKY

(Depth, 53.7 meters; sun altitude, 56.6°)

Tilt angle (Θ)	Azimuth angle (Φ)									
	0	20	40	60	80	100	120	140	160	180
0	202	202	202	202	202	202	202	202	202	202
10	219	218	212	205	194	184	173	163	157	155
20	194	192	180	168	156	143	132	123	116	113
30	139	137	130	120	110	98.8	89.8	82.7	77.6	75.5
40	88.7	87.2	82.9	77.0	70.7	63.9	58.2	53.3	49.9	48.6
50	52.7	52.3	50.1	47.1	43.7	39.6	36.2	33.4	31.2	30.0
60	32.0	31.2	29.6	27.4	25.1	23.1	21.3	19.9	18.8	18.4
70	17.8	17.6	16.9	16.0	14.9	13.8	12.8	12.0	11.4	11.2
80	10.3	10.2	9.87	9.32	8.80	8.28	7.82	7.48	7.14	7.02
90	6.27	6.17	5.98	5.70	5.50	5.27	5.06	4.87	4.67	4.58
100	4.00	3.98	3.91	3.78	3.63	3.49	3.37	3.26	3.18	3.17
110	2.67	2.65	2.63	2.60	2.54	2.46	2.41	2.34	2.31	2.30
120	1.99	1.98	1.97	1.94	1.91	1.86	1.82	1.79	1.76	1.75
130	1.54	1.53	1.53	1.52	1.51	1.48	1.47	1.46	1.45	1.44
140	1.30	1.30	1.30	1.29	1.28	1.28	1.28	1.27	1.27	1.27
150	1.16	1.16	1.16	1.15	1.15	1.15	1.15	1.15	1.15	1.15
160	1.05	1.05	1.05	1.05	1.05	1.05	1.05	1.05	1.05	1.05
170	1.00	1.00	1.00	1.00	1.00	1.00	1.00	1.00	1.00	1.00
180	0.990	0.990	0.990	0.990	0.990	0.990	0.990	0.990	0.990	0.990

TABLE 10

RADIANCE DISTRIBUTION UNDER CLEAR SUNNY SKY
(Depth, 66.1 meters; sun altitude, 56.6°)

Tilt angle (Θ)	Azimuth angle (Φ)									
	0	20	40	60	80	100	120	140	160	180
0	28.8	28.8	28.8	28.8	28.8	28.8	28.8	28.8	28.8	28.8
10	29.8	29.6	29.2	28.4	27.7	26.9	26.1	25.3	24.5	24.1
20	26.1	25.7	24.7	23.8	22.8	21.6	20.6	19.6	18.9	18.5
30	19.7	19.3	18.5	17.5	16.5	15.6	14.6	13.8	13.1	12.8
40	12.7	12.4	11.9	11.3	10.6	10.1	9.44	8.87	8.41	8.19
50	7.64	7.54	7.20	6.83	6.46	6.09	5.70	5.40	5.14	5.01
60	4.43	4.34	4.18	3.98	3.78	3.58	3.38	3.20	3.08	2.98
70	2.46	2.44	2.37	2.29	2.20	2.11	2.01	1.92	1.86	1.81
80	1.43	1.42	1.39	1.35	1.29	1.25	1.19	1.14	1.11	1.09
90	0.858	0.855	0.839	0.817	0.788	0.757	0.727	0.700	0.677	0.661
100	0.531	0.525	0.518	0.506	0.496	0.482	0.468	0.453	0.445	0.439
110	0.357	0.355	0.349	0.342	0.334	0.325	0.317	0.311	0.305	0.301
120	0.252	0.250	0.247	0.244	0.241	0.239	0.235	0.233	0.231	0.226
130	0.186	0.184	0.184	0.181	0.180	0.179	0.177	0.175	0.173	0.172
140	0.146	0.145	0.145	0.144	0.144	0.143	0.142	0.141	0.141	0.139
150	0.124	0.124	0.124	0.122	0.122	0.121	0.121	0.120	0.120	0.120
160	0.108	0.108	0.108	0.108	0.108	0.108	0.108	0.108	0.108	0.108
170	0.100	0.100	0.100	0.100	0.100	0.100	0.100	0.100	0.100	0.100
180	0.0975	0.0975	0.0975	0.0975	0.0975	0.0975	0.0975	0.0975	0.0975	0.0975

(Cox and Munk, 1955), but larger than a single sun image. Owing to the optical state of the surface on 28 April this glitter pattern probably consisted of widely separated points of light. Because of the geometry discussed above it is possible that the solid angle of acceptance never covered more than half of the glitter pattern. This would mean that the reading obtained in the sun's direction could be low by a factor of 2.

In certain directions, and especially at the shallow stations, the presence of the glitter generates a noise signal that varies in both frequency and amplitude as a function of depth. Typical high and low values of this noise, together with its frequency, are given in table 11 for the direction of the sun. In tables 4 through 10 average experimental values for radiance are reported for all directions.

TABLE 11

AMPLITUDE AND FREQUENCY OF THE NOISE SIGNAL IN THE DIRECTION OF THE SUN

Depth (meters)	Maximum variation from mean radiance (%)	Approximate frequency (per min.)
4.2	±93.6	128
10.4	±75.0	74
16.6	±47.4	60
28.9	±10.5	50

DISCUSSION AND TREATMENT OF DATA FOR OVERCAST CONDITIONS

The diffuse nature of the surface lighting for overcast conditions makes it practical to take data during a longer interval around noon than can be used for the clear sunny sky. For the same reason the order in which the stations are run is far less critical. The near-surface data for overcast sky shows the image features of the barge and its shadow at lower contrast than before. The zenith readings at the near-surface stations may exhibit greater variability with an overcast sky because of the time variability in the zenith thickness of the overcast. In addition, the generally lower light level puts the deeper stations experimentally beyond reach. Except for these slight differences the experimental procedure was the same for obtaining the overcast data as it was for obtaining clear sunny data.

The overcast data have been treated by the same procedure used for the clear sunny day data as described in steps 1 through 9, inclusive, with slight modification. Steps 8 and 9 do not, of course, apply as critically to diffuse lighting as they do to the combination of diffuse plus specular lighting provided by a clear sunny day. In step 6, two complete runs of overcast sky data at each depth station were averaged.

DATA FOR OVERCAST CONDITIONS

The voice recorded notes for 16 March, the overcast day, read in part as follows:

> The data from about 1030 on are all excellent overcast data. The instrument was working perfectly. . . . Today's wind velocities ranged from 10 knots at about 1100 to about 2 knots at 1215. At 1400 the water on the south side of the barge where we are operating was as nearly calm as I have seen it. . . .

The radiance distribution data for the overcast condition are given for five depth stations in tables 12 through 16, inclusive.

TABLE 12

RADIANCE DISTRIBUTION, OVERCAST SKY
(Depth, 6.1 meters; sun altitude, 40.0°)

Tilt angle (Θ)	Azimuth angle (Φ)									
	0	20	40	60	80	100	120	140	160	180
0	321,000	321,000	321,000	321,000	321,000	321,000	321,000	321,000	321,000	321,000
10	343,000	342,000	338,000	332,000	325,000	319,000	311,000	306,000	302,000	300,000
20	327,000	326,000	321,000	312,000	302,000	290,000	281,000	272,000	267,000	265,000
30	277,000	275,000	268,000	258,000	243,000	229,000	216,000	207,000	202,000	200,000
40	199,000	196,000	189,000	179,000	167,000	152,000	141,000	132,000	127,000	126,000
50	96,800	95,700	92,500	87,300	81,700	74,900	69,500	65,900	63,600	62,900
60	53,500	52,800	51,100	48,800	45,600	42,800	39,700	37,500	36,100	35,400
70	32,500	32,100	31,300	30,000	28,200	26,100	24,100	22,800	21,900	21,600
80	20,000	19,700	19,100	18,300	17,100	15,800	14,700	13,900	13,500	13,400
90	12,600	12,400	12,000	11,500	10,800	9,950	9,170	8,710	8,380	8,310
100	8,060	7,980	7,780	7,490	7,080	6,640	6,190	5,860	5,670	5,620
110	5,620	5,580	5,450	5,250	4,970	4,670	4,390	4,180	4,050	4,010
120	4,130	4,080	3,990	3,850	3,700	3,500	3,330	3,200	3,120	3,090
130	3,200	3,190	3,150	3,070	2,970	2,860	2,740	2,630	2,570	2,550
140	2,650	2,640	2,590	2,540	2,480	2,390	2,300	2,240	2,190	2,180
150	2,300	2,290	2,280	2,250	2,200	2,150	2,090	2,040	2,000	1,980
160	2,070	2,070	2,060	2,030	2,000	1,960	1,910	1,890	1,890	1,880
170	1,860	1,860	1,860	1,860	1,860	1,860	1,860	1,860	1,860	1,860
180	1,830	1,830	1,830	1,830	1,830	1,830	1,830	1,830	1,830	1,830

TABLE 13

RADIANCE DISTRIBUTION, OVERCAST SKY

(Depth, 18.3 meters; sun altitude, 40.0°)

Tilt angle (Θ)	Azimuth angle (Φ)									
	0	20	40	60	80	100	120	140	160	180
0	26,800	26,800	26,800	26,800	26,800	26,800	26,800	26,800	26,800	26,800
10	27,500	27,400	27,200	26,900	26,600	26,000	25,200	24,600	24,100	23,900
20	23,600	23,400	23,000	22,500	21,900	21,000	20,100	19,400	18,800	18,600
30	17,500	17,400	17,200	16,800	16,200	15,400	14,400	13,400	12,900	12,600
40	11,900	11,800	11,600	11,100	10,600	9,800	9,080	8,460	8,040	7,860
50	7,520	7,460	7,310	7,090	6,750	6,250	5,710	5,240	4,880	4,720
60	4,600	4,540	4,440	4,280	4,070	3,740	3,440	3,230	3,050	2,970
70	2,780	2,750	2,690	2,590	2,450	2,300	2,130	1,990	1,910	1,860
80	1,650	1,640	1,590	1,550	1,470	1,380	1,280	1,220	1,160	1,150
90	1,040	1,020	995	948	892	830	784	745	722	713
100	645	638	627	603	583	557	533	514	502	500
110	454	449	439	426	409	391	378	366	357	356
120	334	331	324	315	302	289	280	272	268	265
130	258	255	250	243	235	228	218	214	209	209
140	206	205	202	198	193	188	185	182	179	179
150	176	175	174	170	167	164	162	161	161	160
160	156	156	156	155	152	151	150	149	147	147
170	145	145	145	145	145	145	145	145	145	145
180	141	141	141	141	141	141	141	141	141	141

TABLE 14

RADIANCE DISTRIBUTION, OVERCAST SKY
(Depth, 30.5 meters; sun altitude, 40.0°)

Tilt angle (Θ)	Azimuth angle (Φ)									
	0	20	40	60	80	100	120	140	160	180
0	2,430	2,430	2,430	2,430	2,430	2,430	2,430	2,430	2,430	2,430
10	2,500	2,490	2,470	2,430	2,380	2,310	2,210	2,120	2,070	2,030
20	2,190	2,170	2,130	2,080	2,010	1,910	1,790	1,680	1,600	1,570
30	1,690	1,670	1,640	1,600	1,550	1,420	1,300	1,180	1,090	1,050
40	1,150	1,130	1,090	1,050	998	927	840	757	702	676
50	688	683	670	649	629	596	544	498	466	453
60	413	409	400	389	375	353	332	302	284	275
70	254	252	247	240	231	217	203	189	178	173
80	153	151	148	144	136	130	121	114	110	108
90	93.9	93.4	91.3	88.6	85.2	81.1	75.9	72.3	69.7	68.4
100	61.2	60.7	59.7	57.9	56.0	53.4	50.6	48.3	46.4	45.3
110	42.9	42.7	41.8	40.7	39.3	37.8	35.8	34.2	33.3	32.7
120	31.1	30.9	30.5	29.8	29.1	28.1	27.2	26.3	25.8	25.4
130	23.8	23.7	23.5	23.1	22.8	22.2	21.6	21.2	21.0	20.9
140	20.4	20.3	20.0	19.8	19.5	19.0	18.4	18.1	17.6	17.5
150	18.1	18.0	17.8	17.5	17.3	16.9	16.7	16.5	16.3	16.3
160	16.2	16.1	16.1	16.1	16.0	15.8	15.5	15.3	15.2	15.2
170	14.9	14.9	14.9	14.9	14.9	14.9	14.9	14.9	14.9	14.9
180	14.8	14.8	14.8	14.8	14.8	14.8	14.8	14.8	14.8	14.8

TABLE 15

RADIANCE DISTRIBUTION, OVERCAST SKY
(Depth, 42.8 meters; sun altitude, 40.0°)

Tilt angle (Θ)	Azimuth angle (Φ)									
	0	20	40	60	80	100	120	140	160	180
0	250	250	250	250	250	250	250	250	250	250
10	254	252	250	247	242	239	233	227	223	221
20	229	226	223	216	209	201	190	182	176	174
30	175	173	167	161	155	146	138	131	125	123
40	119	117	113	109	104	99.1	92.5	87.4	83.9	82.6
50	76.0	74.9	73.4	70.4	67.0	63.6	59.8	56.9	54.7	53.8
60	45.7	45.3	44.0	42.6	40.8	39.1	38.2	36.6	35.4	34.9
70	27.6	27.2	26.6	25.9	24.9	24.0	22.9	22.0	21.2	20.9
80	16.8	16.6	16.2	15.8	15.4	14.7	14.1	13.6	13.2	13.1
90	10.5	10.4	10.1	9.87	9.55	9.21	8.87	8.58	8.38	8.20
100	6.82	6.78	6.61	6.48	6.28	6.06	5.82	5.61	5.40	5.35
110	4.66	4.63	4.55	4.46	4.36	4.24	4.08	3.95	3.86	3.82
120	3.46	3.42	3.39	3.33	3.27	3.16	3.08	3.02	2.96	2.94
130	2.67	2.66	2.65	2.61	2.58	2.52	2.45	2.39	2.34	2.32
140	2.22	2.22	2.20	2.16	2.13	2.10	2.06	2.01	1.99	1.97
150	1.93	1.93	1.93	1.92	1.91	1.89	1.88	1.86	1.83	1.82
160	1.76	1.76	1.76	1.76	1.76	1.76	1.76	1.76	1.76	1.76
170	1.67	1.67	1.67	1.67	1.67	1.67	1.67	1.67	1.67	1.67
180	1.65	1.65	1.65	1.65	1.65	1.65	1.65	1.65	1.65	1.65

TABLE 16

RADIANCE DISTRIBUTION, OVERCAST SKY

(Depth, 55.0 meters; sun altitude, 40.0°)

Tilt angle (Θ)	Azimuth angle (Φ)									
	0	20	40	60	80	100	120	140	160	180
0	29.6	29.6	29.6	29.6	29.6	29.6	29.6	29.6	29.6	29.6
10	29.9	29.7	29.3	28.8	28.2	27.6	27.0	26.5	25.9	25.7
20	24.7	24.6	24.0	23.4	22.8	22.2	21.5	20.9	20.5	20.4
30	18.8	18.5	18.1	17.7	17.3	16.6	16.0	15.4	14.9	14.6
40	13.0	12.8	12.6	12.3	11.9	11.6	11.2	10.8	10.5	10.4
50	8.11	8.00	7.86	7.72	7.54	7.32	7.07	6.86	6.69	6.61
60	4.99	4.96	4.85	4.76	4.64	4.55	4.42	4.28	4.19	4.17
70	3.00	2.98	2.93	2.87	2.81	2.75	2.69	2.63	2.59	2.56
80	1.90	1.88	1.84	1.82	1.78	1.75	1.71	1.67	1.65	1.63
90	1.19	1.18	1.16	1.15	1.12	1.09	1.07	1.05	1.04	1.03
100	0.765	0.761	0.749	0.736	0.723	0.708	0.689	0.678	0.665	0.661
110	0.512	0.509	0.503	0.495	0.488	0.481	0.469	0.460	0.452	0.449
120	0.363	0.360	0.358	0.355	0.352	0.346	0.341	0.337	0.333	0.331
130	0.273	0.272	0.271	0.268	0.266	0.264	0.259	0.256	0.254	0.253
140	0.215	0.215	0.214	0.213	0.210	0.208	0.206	0.204	0.203	0.203
150	0.181	0.181	0.181	0.181	0.181	0.181	0.181	0.181	0.181	0.181
160	0.158	0.158	0.158	0.158	0.158	0.158	0.158	0.158	0.158	0.158
170	0.146	0.146	0.146	0.146	0.146	0.146	0.146	0.146	0.146	0.146
180	0.143	0.143	0.143	0.143	0.143	0.143	0.143	0.143	0.143	0.143

DISCUSSION OF DATA AND EVALUATION OF SOURCES OF ERROR

The data presented in tables 12 through 16 are correct to better than ±5 per cent of the listed value at each entry. Noise due to wave action, and excessive errors in the direction of the sun, are not manifest in the overcast data.

ASYMPTOTIC RADIANCE DISTRIBUTION

It has long been conjectured and perhaps first clearly stated by Whitney (1941*a*, *b*) that the radiance distribution in an optically deep and homogeneous hydrosol approaches a characteristic shape with increasing depth. This final distribution is referred to as the asymptotic radiance distribution because of the manner of its approach to the final shape. Recently Preisendorfer (1958*a*, *b*) has developed a proof of the existence of asymptotic radiance distribution which shows that the final shape depends only on the inherent optical properties of the hydrosol, i.e., the volume scattering function and the absorption coefficient. It is independent of the lighting conditions at the surface of the water and of the optical state of the water surface. As the absorption coefficient approaches zero in a scattering-absorbing medium the asymptotic radiance distribution tends to become a sphere, whereas if the scattering coefficient approaches zero the final shape tends to be a vertical line. In between these limits there will be an infinite variety of prolate surfaces of revolution oriented with the poles along the vertical axis, each one characteristic of the inherent optical properties of a particular hydrosol.

The transformation of radiance distribution from the complex structure found near the surface to its final symmetrical shape at great depth will require enhancement of radiance in some directions, attenuation in others.

This is evident in the data shown in figure 2 and to some extent in the tables of radiance data, and can be deduced from theory in the following way. Starting with the equation of transfer for radiance (1), see Preisendorfer (1958*a*),

$$\cos\Theta \frac{dN(Z,\Theta,\Phi)}{dZ} = -\alpha(Z)N(Z,\Theta,\Phi) + N_*(Z,\Theta,\Phi) \tag{1}$$

where Θ is the azimuth angle from the zenith
Φ is the azimuth angle from the sun
Z is the depth
N is the radiance
α is the total attenuation coefficient
N_* is the path function

dN, N, and N_* are all taken at the same depth (Z) and in the same direction (Θ, Φ).

We note that the attenuation coefficient (K) for radiance for this same depth and direction is by definition

$$K(Z,\Theta,\Phi) = -\frac{1}{N(Z,\Theta,\Phi)} \frac{dN(Z,\Theta,\Phi)}{dZ}. \tag{2}$$

Thus

$$(\cos\Theta)K(Z,\Theta,\Phi) = \alpha(Z) - \frac{N_*(Z,\Theta,\Phi)}{N(Z,\Theta,\Phi)}. \tag{3}$$

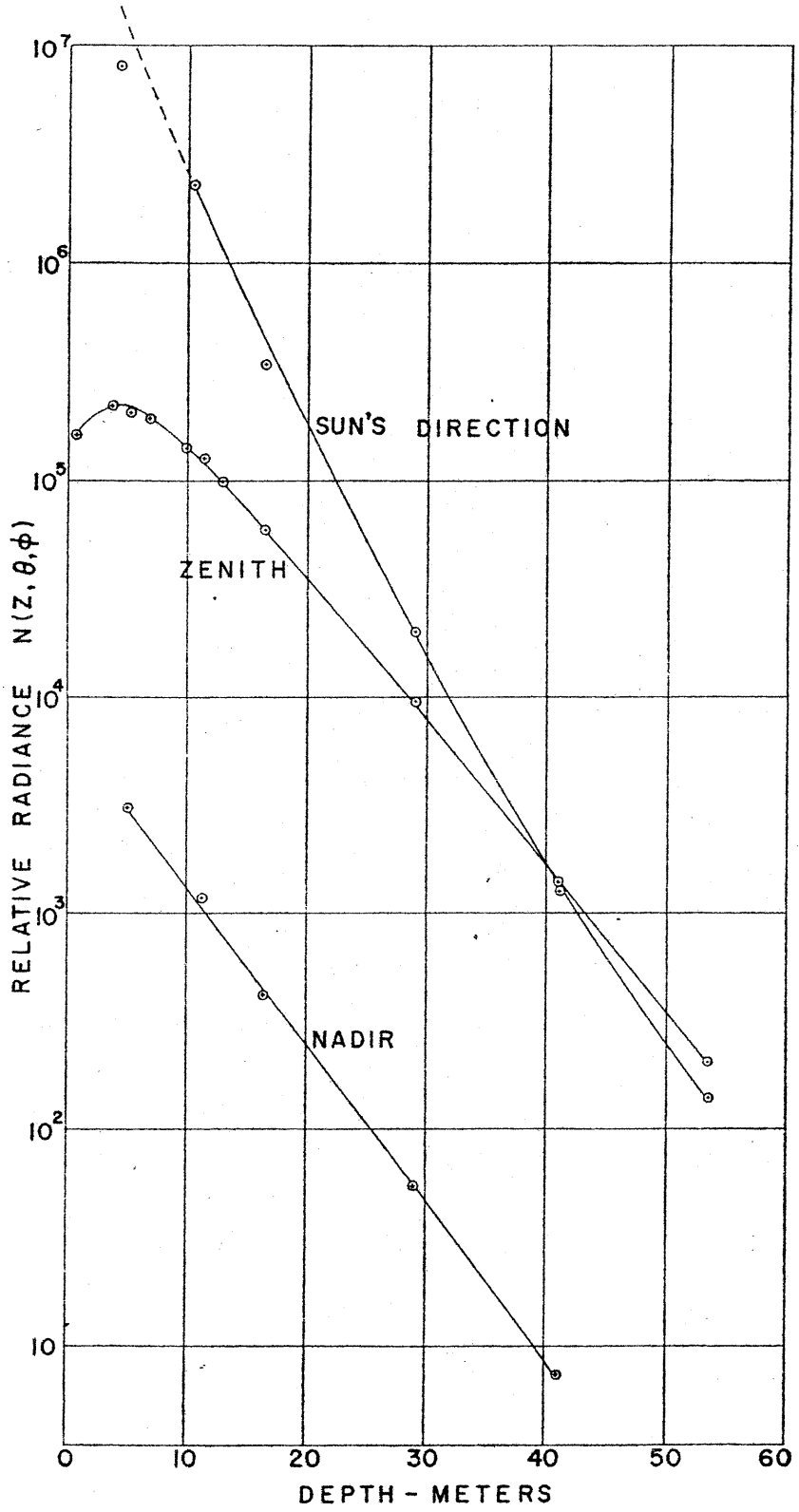
10^7
10^6
10^5
10^4
10^3
10^2
10
SUN'S DIRECTION
ZENITH
NADIR
RELATIVE RADIANCE N(Z, θ, φ)
0
10
20
30
40
50
60
DEPTH - METERS

Figure 2

By definition

$$N_*(Z, \Theta, \Phi) = \int_{\substack{\text{over all} \\ \text{directions}}} \sigma(Z, \Theta, \Phi, \Theta', \Phi') N(Z, \Theta', \Phi')\, d\Omega$$

where the volume scattering function σ has direction Θ, Φ for incident radiance in the direction Θ', Φ'. For shallow depths the sun is by far the most important contribution to N_* and we can let Θ', Φ' describe the incident radiance from the sun only, that is,

$$\Theta' = \Theta_S$$
$$\Phi' = \Phi_S$$
$$N = N_S$$

and the solid angle $\Omega = \Omega_S$, the solid angle of the sun.

Then $N_*(Z, \Theta, \Phi)$ may be approximated by the equation

$$N_*(Z, \Theta, \Phi) = \sigma(Z, \Theta, \Phi, \Theta_S, \Phi_S)\, N_S \Omega_S .$$

Equation (3) can thus be written

$$K(Z, \Theta, \Phi) \cong \frac{1}{\cos \Theta} \left[\alpha(Z) - \frac{\sigma(Z, \Theta, \Phi, \Theta_S) N_S\, \Omega_S}{N(Z, \Theta, \Phi_S)} \right] . \tag{4}$$

For the three directions illustrated in figure 2 specific values of Θ and Φ can be assigned as shown below; and the negative slope, K, of the curves of figure 2 can be roughly predicted for a fixed depth Z near the surface by equations 5, 6, and 7.

Direction	Θ	Φ	$N(Z, \Theta, \Phi)$	$\sigma(Z, \Theta, \Phi, \Theta_S, \Phi_S)$
Zenith.....	0	0	N_{zenith}	24° forward scattering = σ_{24}
Sun.....	Θ_S	Φ_S	N_{sun}	forward scattering within the beam = σ_0
Nadir.....	π	0	N_{nadir}	156° backward scattering = σ_{156}

(The underwater angle of the sun from the zenith (Θ_S) for the clear sunny day data presented in this report is about 24°.)

$$K_{zenith} = \alpha - \frac{\sigma_{24} N_S\, \Omega_S}{N_{zenith}} \tag{5}$$

$$K_{sun} = \frac{1}{\cos \Theta_S} \left[\alpha - \frac{\sigma_0 N_S\, \Omega_S}{N_S} \right] \tag{6}$$

$$K_{nadir} = - \left[\alpha - \frac{\sigma_{156} N_S\, \Omega_S}{N_{nadir}} \right] \tag{7}$$

It can be seen from equation 5 that when N_{zenith} is sufficiently dark, as it is when seen from a depth of less than 4 m at Lake Pend Oreille on a clear sunny day, the

second term on the right of the equation will be larger than α and a positive slope will result in figure 2. With increasing depth N_{zenith} increases until the two terms on the right of equation 5 are equal and the slope becomes zero.

In the direction of the sun (eq. 6) the second term on the right of the equation will be minimized owing to the presence of N_S in the denominator. The slope in figure 2 will therefore be negative and maximum near the surface as shown but will become smaller as N_S decreases with depth.

In the nadir direction (eq. 7) the second term will always be larger than α but the change in sign ensures that the slope of the curve in figure 2 will always be negative. Also since the ratio N_S/N_{nadir} will not change greatly with depth, the value of K would be expected to remain nearly constant.

From this brief example the value of radiance K data in following and predicting the changes in shape of the radiance distribution solid as a function of depth can easily be seen. By means of radiance K data the radiance distribution at other depths can be extrapolated and a quantitative estimate of the proximity to asymptotic distribution can be obtained.

Radiance K data for clear sunny conditions are given in tables 17 through 23, and for overcast conditions, in tables 24 through 28.

TABLE 17

RADIANCE *K* VALUES, CLEAR SUNNY SKY
(Depth, 7.33 meters; sun altitude, 56.6°)

Tilt angle (Θ)	Azimuth angle (Φ)									
	0	20	40	60	80	100	120	140	160	180
0	0.0764	0.0764	0.0764	0.0764	0.0764	0.0764	0.0764	0.0764	0.0764	0.0764
10	0.110	0.101	0.0896	0.0879	0.0863	0.0846	0.0846	0.0676	0.0627	0.0607
20	0.127	0.125	0.105	0.0909	0.0824	0.0804	0.0784	0.0764	0.0712	0.0679
30	0.185	0.136	0.106	0.0958	0.0942	0.0925	0.0932	0.0942	0.0919	0.0886
40	0.106	0.117	0.112	0.105	0.106	0.111	0.117	0.122	0.126	0.131
50	0.0912	0.0751	0.0682	0.0679	0.0738	0.0817	0.0912	0.0945	0.0919	0.0942
60	0.115	0.0948	0.0791	0.0794	0.0906	0.100	0.106	0.110	0.109	0.111
70	0.104	0.101	0.103	0.106	0.114	0.119	0.124	0.125	0.125	0.121
80	0.134	0.130	0.124	0.129	0.135	0.137	0.133	0.138	0.136	0.133
90	0.150	0.149	0.147	0.149	0.150	0.149	0.147	0.143	0.138	0.134
100	0.156	0.155	0.150	0.144	0.148	0.151	0.151	0.149	0.147	0.144
110	0.155	0.154	0.147	0.144	0.148	0.155	0.157	0.158	0.156	0.155
120	0.154	0.152	0.150	0.147	0.150	0.158	0.161	0.163	0.163	0.161
130	0.158	0.157	0.153	0.151	0.152	0.150	0.153	0.153	0.155	0.155
140	0.154	0.153	0.150	0.150	0.149	0.151	0.152	0.153	0.155	0.155
150	0.152	0.151	0.151	0.151	0.152	0.152	0.153	0.153	0.155	0.154
160	0.157	0.157	0.157	0.157	0.157	0.157	0.157	0.157	0.156	0.156
170	0.156	0.156	0.156	0.156	0.156	0.156	0.156	0.156	0.156	0.156
180	0.154	0.154	0.154	0.154	0.154	0.154	0.154	0.154	0.154	0.154

TABLE 18

RADIANCE *K* VALUES, CLEAR SUNNY SKY
(Depth, 10.42 meters; sun altitude, 56.6°)

Tilt angle (Θ)	Azimuth angle (Φ)									
	0	20	40	60	80	100	120	140	160	180
0	0.100	0.100	0.100	0.100	0.100	0.100	0.100	0.100	0.100	0.100
10	0.121	0.119	0.113	0.110	0.106	0.103	0.0991	0.0958	0.0939	0.0925
20	0.197	0.160	0.131	0.110	0.0994	0.0945	0.0942	0.0958	0.0968	0.0961
30	0.246	0.152	0.125	0.107	0.0991	0.0965	0.0994	0.103	0.107	0.108
40	0.151	0.140	0.121	0.108	0.106	0.109	0.115	0.126	0.125	0.127
50	0.122	0.114	0.0988	0.0951	0.0971	0.101	0.105	0.110	0.114	0.117
60	0.125	0.115	0.110	0.110	0.111	0.112	0.114	0.119	0.119	0.122
70	0.131	0.131	0.131	0.127	0.126	0.125	0.131	0.129	0.130	0.129
80	0.148	0.146	0.142	0.140	0.138	0.136	0.133	0.136	0.137	0.137
90	0.154	0.155	0.153	0.150	0.146	0.144	0.144	0.144	0.146	0.145
100	0.160	0.158	0.155	0.151	0.151	0.151	0.151	0.151	0.151	0.150
110	0.162	0.160	0.157	0.155	0.154	0.153	0.155	0.155	0.154	0.154
120	0.163	0.160	0.158	0.156	0.157	0.157	0.158	0.158	0.157	0.157
130	0.161	0.159	0.157	0.157	0.157	0.156	0.157	0.157	0.158	0.158
140	0.160	0.159	0.158	0.158	0.158	0.159	0.159	0.159	0.159	0.158
150	0.159	0.159	0.159	0.158	0.159	0.158	0.159	0.159	0.159	0.159
160	0.160	0.161	0.161	0.159	0.161	0.161	0.162	0.163	0.163	0.163
170	0.162	0.162	0.162	0.162	0.162	0.162	0.162	0.162	0.162	0.162
180	0.162	0.162	0.162	0.162	0.162	0.162	0.162	0.162	0.162	0.162

TABLE 19

RADIANCE *K* VALUES, CLEAR SUNNY SKY
(Depth, 16.58 meters; sun altitude, 56.6°)

Tilt angle (Θ)	Azimuth angle (Φ)									
	0	20	40	60	80	100	120	140	160	180
0	0.123	0.123	0.123	0.123	0.123	0.123	0.123	0.123	0.123	0.123
10	0.147	0.145	0.139	0.133	0.127	0.123	0.118	0.115	0.115	0.115
20	0.214	0.178	0.154	0.136	0.125	0.117	0.115	0.114	0.115	0.115
30	0.243	0.178	0.152	0.136	0.125	0.119	0.116	0.117	0.119	0.120
40	0.164	0.160	0.148	0.136	0.128	0.125	0.125	0.126	0.129	0.131
50	0.150	0.145	0.136	0.127	0.121	0.118	0.119	0.121	0.125	0.128
60	0.152	0.147	0.141	0.135	0.130	0.127	0.124	0.126	0.129	0.131
70	0.153	0.152	0.150	0.144	0.140	0.137	0.136	0.135	0.136	0.137
80	0.160	0.160	0.157	0.153	0.149	0.146	0.142	0.142	0.142	0.142
90	0.164	0.164	0.160	0.157	0.153	0.150	0.148	0.147	0.148	0.149
100	0.165	0.164	0.162	0.159	0.156	0.154	0.153	0.152	0.152	0.152
110	0.165	0.164	0.162	0.152	0.156	0.156	0.156	0.155	0.156	0.156
120	0.162	0.162	0.162	0.160	0.159	0.158	0.159	0.159	0.160	0.160
130	0.161	0.161	0.161	0.160	0.160	0.160	0.160	0.160	0.160	0.160
140	0.161	0.161	0.161	0.161	0.161	0.160	0.160	0.161	0.161	0.161
150	0.161	0.161	0.161	0.161	0.161	0.161	0.161	0.161	0.161	0.161
160	0.161	0.162	0.162	0.162	0.162	0.163	0.163	0.163	0.163	0.163
170	0.163	0.163	0.163	0.163	0.163	0.163	0.163	0.163	0.163	0.163
180	0.163	0.163	0.163	0.163	0.163	0.163	0.163	0.163	0.163	0.163

TABLE 20

RADIANCE *K* VALUES, CLEAR SUNNY SKY
(Depth, 29.0 meters; sun altitude, 56.6°)

Tilt angle (Θ)	Azimuth angle (Φ)									
	0	20	40	60	80	100	120	140	160	180
0	0.152	0.152	0.152	0.152	0.152	0.152	0.152	0.152	0.152	0.152
10	0.174	0.172	0.167	0.160	0.154	0.148	0.143	0.141	0.140	0.140
20	0.216	0.192	0.176	0.163	0.153	0.145	0.140	0.137	0.136	0.137
30	0.232	0.201	0.178	0.164	0.154	0.146	0.141	0.137	0.137	0.136
40	0.136	0.188	0.176	0.164	0.155	0.148	0.142	0.136	0.136	0.136
50	0.182	0.180	0.175	0.164	0.154	0.147	0.140	0.138	0.136	0.136
60	0.178	0.175	0.171	0.163	0.156	0.150	0.146	0.144	0.142	0.142
70	0.175	0.173	0.168	0.164	0.159	0.154	0.148	0.147	0.146	0.145
80	0.176	0.175	0.172	0.167	0.162	0.158	0.154	0.151	0.149	0.148
90	0.177	0.175	0.171	0.167	0.163	0.159	0.155	0.153	0.151	0.151
100	0.172	0.172	0.171	0.167	0.163	0.160	0.157	0.156	0.155	0.155
110	0.172	0.171	0.169	0.166	0.164	0.162	0.159	0.158	0.158	0.158
120	0.168	0.168	0.167	0.165	0.164	0.162	0.161	0.161	0.161	0.161
130	0.166	0.166	0.165	0.165	0.164	0.163	0.162	0.161	0.161	0.161
140	0.165	0.164	0.164	0.164	0.163	0.163	0.162	0.161	0.162	0.163
150	0.164	0.164	0.164	0.164	0.163	0.163	0.163	0.162	0.162	0.162
160	0.164	0.164	0.164	0.164	0.163	0.163	0.163	0.162	0.162	0.162
170	0.163	0.163	0.163	0.163	0.163	0.163	0.163	0.163	0.163	0.163
180	0.163	0.163	0.163	0.163	0.163	0.163	0.163	0.163	0.163	0.163

TABLE 21

RADIANCE *K* VALUES, CLEAR SUNNY SKY
(Depth, 41.3 meters; sun altitude, 56.6°)

Tilt angle (Θ)	Azimuth angle (Φ)									
	0	20	40	60	80	100	120	140	160	180
0	0.156	0.156	0.156	0.156	0.156	0.156	0.156	0.156	0.156	0.156
10	0.169	0.166	0.163	0.159	0.157	0.155	0.153	0.151	0.149	0.148
20	0.191	0.179	0.170	0.163	0.158	0.154	0.151	0.148	0.145	0.144
30	0.200	0.185	0.172	0.164	0.158	0.155	0.152	0.149	0.146	0.144
40	0.191	0.183	0.174	0.166	0.161	0.157	0.154	0.150	0.145	0.143
50	0.185	0.181	0.174	0.168	0.163	0.159	0.155	0.149	0.144	0.141
60	0.180	0.177	0.172	0.167	0.164	0.160	0.156	0.151	0.147	0.144
70	0.178	0.175	0.170	0.167	0.163	0.158	0.157	0.153	0.149	0.147
80	0.176	0.173	0.170	0.167	0.164	0.161	0.158	0.155	0.152	0.149
90	0.174	0.173	0.171	0.168	0.165	0.161	0.158	0.155	0.152	0.151
100	0.173	0.171	0.169	0.166	0.164	0.162	0.162	0.157	0.155	0.154
110	0.172	0.171	0.169	0.166	0.165	0.163	0.161	0.159	0.157	0.157
120	0.170	0.170	0.167	0.165	0.164	0.163	0.161	0.160	0.158	0.158
130	0.168	0.168	0.166	0.165	0.164	0.163	0.162	0.161	0.160	0.160
140	0.167	0.166	0.165	0.164	0.164	0.163	0.162	0.162	0.161	0.160
150	0.165	0.165	0.164	0.164	0.163	0.162	0.162	0.161	0.161	0.160
160	0.164	0.164	0.163	0.163	0.163	0.162	0.162	0.162	0.162	0.162
170	0.163	0.163	0.163	0.163	0.163	0.163	0.163	0.163	0.163	0.163
180	0.163	0.163	0.163	0.163	0.163	0.163	0.163	0.163	0.163	0.163

TABLE 22

RADIANCE K VALUES, CLEAR SUNNY SKY
(Depth, 53.7 meters; sun altitude, 56.6°)

Tilt angle (Θ)	Azimuth angle (Φ)									
	0	20	40	60	80	100	120	140	160	180
0	0.156	0.156	0.156	0.156	0.156	0.156	0.156	0.156	0.156	0.156
10	0.163	0.161	0.159	0.157	0.156	0.155	0.154	0.153	0.153	0.152
20	0.168	0.166	0.163	0.160	0.157	0.154	0.153	0.151	0.149	0.148
30	0.168	0.166	0.163	0.160	0.157	0.154	0.152	0.149	0.147	0.146
40	0.170	0.168	0.164	0.161	0.158	0.155	0.152	0.150	0.147	0.146
50	0.169	0.167	0.165	0.162	0.159	0.157	0.154	0.151	0.148	0.147
60	0.170	0.169	0.166	0.162	0.159	0.156	0.153	0.150	0.147	0.146
70	0.169	0.168	0.166	0.162	0.159	0.156	0.154	0.150	0.148	0.147
80	0.166	0.165	0.163	0.161	0.159	0.157	0.155	0.154	0.151	0.150
90	0.165	0.164	0.163	0.163	0.161	0.158	0.157	0.156	0.155	0.155
100	0.167	0.166	0.165	0.163	0.161	0.160	0.159	0.158	0.157	0.156
110	0.166	0.165	0.165	0.164	0.163	0.162	0.162	0.161	0.160	0.159
120	0.167	0.167	0.167	0.166	0.165	0.164	0.163	0.162	0.161	0.161
130	0.169	0.168	0.169	0.168	0.168	0.168	0.167	0.167	0.166	0.166
140	0.172	0.172	0.171	0.171	0.171	0.171	0.171	0.170	0.170	0.169
150	0.172	0.172	0.172	0.172	0.172	0.172	0.172	0.172	0.172	0.171
160	0.174	0.174	0.174	0.174	0.174	0.174	0.174	0.174	0.174	0.174
170	0.175	0.175	0.175	0.175	0.175	0.175	0.175	0.175	0.175	0.175
180	0.176	0.176	0.176	0.176	0.176	0.176	0.176	0.176	0.176	0.176

TABLE 23

RADIANCE *K* VALUES, CLEAR SUNNY SKY

(Depth, 59.9 meters; sun altitude, 56.6°)

Tilt angle (Θ)	Azimuth angle (Φ)									
	0	20	40	60	80	100	120	140	160	180
0	0.157	0.157	0.157	0.157	0.157	0.157	0.157	0.157	0.157	0.157
10	0.161	0.161	0.160	0.160	0.157	0.156	0.153	0.151	0.150	0.150
20	0.162	0.162	0.160	0.158	0.155	0.153	0.150	0.149	0.147	0.147
30	0.158	0.159	0.158	0.156	0.153	0.149	0.147	0.145	0.144	0.143
40	0.157	0.157	0.157	0.156	0.150	0.149	0.147	0.145	0.144	0.144
50	0.156	0.157	0.157	0.156	0.155	0.151	0.149	0.147	0.146	0.145
60	0.159	0.159	0.158	0.155	0.153	0.151	0.149	0.148	0.146	0.147
70	0.159	0.159	0.159	0.157	0.155	0.153	0.150	0.148	0.147	0.147
80	0.159	0.159	0.158	0.156	0.155	0.153	0.152	0.152	0.150	0.150
90	0.160	0.159	0.158	0.157	0.157	0.157	0.157	0.157	0.156	0.157
100	0.163	0.163	0.163	0.162	0.161	0.160	0.159	0.159	0.159	0.160
110	0.162	0.163	0.163	0.164	0.164	0.164	0.164	0.163	0.164	0.164
120	0.167	0.167	0.168	0.168	0.167	0.166	0.165	0.165	0.164	0.166
130	0.171	0.171	0.172	0.172	0.172	0.171	0.172	0.172	0.172	0.172
140	0.177	0.178	0.178	0.178	0.178	0.178	0.178	0.178	0.178	0.179
150	0.181	0.181	0.181	0.181	0.181	0.182	0.182	0.183	0.183	0.182
160	0.184	0.184	0.184	0.184	0.184	0.184	0.184	0.184	0.184	0.184
170	0.187	0.187	0.187	0.187	0.187	0.187	0.187	0.187	0.187	0.187
180	0.188	0.188	0.188	0.188	0.188	0.188	0.188	0.188	0.188	0.188

TABLE 24

RADIANCE K VALUES, OVERCAST SKY
(Depth, 12.2 meters; sun altitude, 40.0°)

Tilt angle (Θ)	Azimuth angle (Φ)									
	0	20	40	60	80	100	120	140	160	180
0	0.204	0.204	0.204	0.204	0.204	0.204	0.204	0.204	0.204	0.204
10	0.207	0.207	0.206	0.206	0.205	0.206	0.206	0.207	0.207	0.207
20	0.215	0.216	0.216	0.215	0.214	0.215	0.216	0.217	0.218	0.218
30	0.226	0.226	0.225	0.224	0.222	0.222	0.223	0.224	0.224	0.226
40	0.230	0.230	0.228	0.228	0.226	0.225	0.225	0.225	0.226	0.227
50	0.209	0.209	0.208	0.206	0.204	0.204	0.205	0.208	0.210	0.212
60	0.201	0.201	0.200	0.199	0.198	0.200	0.200	0.201	0.203	0.203
70	0.201	0.201	0.201	0.201	0.200	0.199	0.199	0.200	0.200	0.201
80	0.204	0.203	0.204	0.202	0.201	0.200	0.200	0.200	0.201	0.201
90	0.204	0.204	0.204	0.204	0.204	0.203	0.201	0.201	0.201	0.201
100	0.207	0.207	0.206	0.206	0.205	0.203	0.201	0.199	0.199	0.198
110	0.206	0.206	0.206	0.206	0.205	0.203	0.201	0.200	0.199	0.199
120	0.206	0.206	0.205	0.205	0.205	0.204	0.203	0.202	0.201	0.201
130	0.206	0.207	0.207	0.208	0.208	0.207	0.207	0.205	0.205	0.205
140	0.209	0.209	0.208	0.209	0.209	0.208	0.206	0.206	0.205	0.205
150	0.210	0.210	0.210	0.211	0.211	0.210	0.209	0.208	0.206	0.206
160	0.211	0.211	0.211	0.210	0.210	0.209	0.208	0.208	0.209	0.208
170	0.209	0.209	0.209	0.209	0.209	0.209	0.209	0.209	0.209	0.209
180	0.209	0.209	0.209	0.209	0.209	0.209	0.209	0.209	0.209	0.209

TABLE 25

RADIANCE *K* VALUES, OVERCAST SKY
(Depth, 18.3 meters; sun altitude, 40.0°)

Tilt angle (Θ)	Azimuth angle (Φ)									
	0	20	40	60	80	100	120	140	160	180
0	0.200	0.200	0.200	0.200	0.200	0.200	0.200	0.200	0.200	0.200
10	0.201	0.202	0.201	0.201	0.201	0.202	0.203	0.204	0.204	0.205
20	0.205	0.205	0.205	0.205	0.205	0.206	0.207	0.208	0.209	0.210
30	0.208	0.208	0.208	0.208	0.207	0.208	0.209	0.212	0.214	0.215
40	0.211	0.211	0.211	0.210	0.210	0.208	0.210	0.211	0.212	0.214
50	0.202	0.202	0.201	0.201	0.199	0.198	0.199	0.200	0.201	0.202
60	0.199	0.199	0.199	0.198	0.197	0.196	0.196	0.197	0.198	0.199
70	0.198	0.198	0.198	0.198	0.197	0.196	0.196	0.196	0.197	0.197
80	0.199	0.199	0.199	0.198	0.198	0.197	0.196	0.197	0.196	0.197
90	0.200	0.200	0.200	0.199	0.198	0.197	0.196	0.196	0.196	0.196
100	0.199	0.199	0.199	0.199	0.198	0.197	0.197	0.196	0.197	0.197
110	0.199	0.199	0.199	0.199	0.198	0.197	0.197	0.197	0.196	0.197
120	0.200	0.200	0.199	0.199	0.198	0.197	0.196	0.196	0.196	0.196
130	0.200	0.200	0.200	0.200	0.199	0.198	0.198	0.197	0.196	0.196
140	0.199	0.199	0.198	0.198	0.198	0.197	0.197	0.197	0.197	0.197
150	0.198	0.198	0.198	0.198	0.198	0.198	0.197	0.197	0.196	0.196
160	0.198	0.198	0.198	0.197	0.197	0.197	0.196	0.196	0.197	0.197
170	0.197	0.197	0.197	0.197	0.197	0.197	0.197	0.197	0.197	0.197
180	0.196	0.196	0.196	0.196	0.196	0.196	0.196	0.196	0.196	0.196

TABLE 26

RADIANCE *K* VALUES, OVERCAST SKY

(Depth, 30.5 meters; sun altitude, 40.0°)

Tilt angle (Θ)	Azimuth angle (Φ)									
	0	20	40	60	80	100	120	140	160	180
0	0.191	0.191	0.191	0.191	0.191	0.191	0.191	0.191	0.191	0.191
10	0.192	0.192	0.192	0.192	0.192	0.192	0.191	0.192	0.191	0.191
20	0.189	0.190	0.190	0.190	0.190	0.190	0.191	0.191	0.191	0.191
30	0.188	0.189	0.189	0.190	0.190	0.190	0.189	0.189	0.190	0.189
40	0.188	0.189	0.189	0.189	0.189	0.188	0.187	0.187	0.186	0.186
50	0.188	0.188	0.188	0.188	0.188	0.187	0.186	0.185	0.183	0.183
60	0.188	0.188	0.188	0.188	0.188	0.186	0.184	0.183	0.182	0.182
70	0.188	0.189	0.188	0.188	0.187	0.186	0.185	0.184	0.184	0.183
80	0.187	0.188	0.187	0.187	0.186	0.185	0.184	0.183	0.183	0.183
90	0.188	0.187	0.187	0.186	0.185	0.184	0.183	0.182	0.182	0.182
100	0.186	0.185	0.186	0.185	0.185	0.184	0.184	0.184	0.185	0.185
110	0.187	0.187	0.186	0.186	0.185	0.185	0.185	0.185	0.185	0.185
120	0.186	0.187	0.186	0.186	0.183	0.184	0.184	0.184	0.183	0.184
130	0.186	0.186	0.185	0.185	0.184	0.184	0.183	0.183	0.183	0.184
140	0.185	0.185	0.185	0.185	0.184	0.184	0.183	0.184	0.184	0.184
150	0.184	0.184	0.184	0.183	0.182	0.182	0.182	0.182	0.183	0.183
160	0.183	0.183	0.183	0.183	0.182	0.182	0.182	0.181	0.181	0.181
170	0.182	0.182	0.182	0.182	0.182	0.182	0.182	0.182	0.182	0.182
180	0.182	0.182	0.182	0.182	0.182	0.182	0.182	0.182	0.182	0.182

TABLE 27

RADIANCE K VALUES, OVERCAST SKY

(Depth, 42.8 meters; sun altitude, 40.0°)

Tilt angle (Θ)	Azimuth angle (Φ)									
	0	20	40	60	80	100	120	140	160	180
0	0.180	0.180	0.180	0.180	0.180	0.180	0.180	0.180	0.180	0.180
10	0.181	0.181	0.181	0.181	0.181	0.181	0.180	0.179	0.179	0.179
20	0.183	0.183	0.183	0.183	0.183	0.182	0.181	0.179	0.178	0.177
30	0.184	0.184	0.184	0.184	0.184	0.182	0.180	0.177	0.175	0.175
40	0.183	0.183	0.182	0.182	0.181	0.179	0.176	0.174	0.172	0.171
50	0.181	0.182	0.182	0.181	0.181	0.180	0.177	0.175	0,173	0.173
60	0.180	0.180	0.180	0.180	0.179	0.178	0.176	0.174	0.172	0.171
70	0.181	0.181	0.181	0.181	0.180	0.178	0.177	0.175	0.173	0.172
80	0.179	0.179	0.179	0.178	0.177	0.176	0.174	0.172	0.172	0.171
90	0.178	0.178	0.178	0.178	0.177	0.176	0.174	0.173	0.172	0.171
100	0.179	0.179	0.179	0.178	0.178	0.177	0.175	0.174	0.173	0.172
110	0.181	0.181	0.181	0.180	0.179	0.178	0.177	0.177	0.176	0.175
120	0.182	0.182	0.182	0.181	0.180	0.180	0.179	0.178	0.178	0.177
130	0.183	0.183	0.182	0.182	0.182	0.181	0.181	0.181	0.180	0.180
140	0.186	0.186	0.186	0.185	0.185	0.185	0.184	0.183	0.183	0.182
150	0.188	0.188	0.188	0.187	0.187	0.186	0.185	0.185	0.184	0.184
160	0.190	0.189	0.189	0.189	0.189	0.188	0.188	0.187	0.187	0.187
170	0.190	0.190	0.190	0.190	0.190	0.190	0.190	0.190	0.190	0.190
180	0.190	0.190	0.190	0.190	0.190	0.190	0.190	0.190	0.190	0.190

TABLE 28

RADIANCE K VALUES, OVERCAST SKY

(Depth, 48.9 meters; sun altitude, 40.0°)

Tilt angle (θ)	Azimuth angle (Φ)									
	0	20	40	60	80	100	120	140	160	180
0	0.175	0.175	0.175	0.175	0.175	0.175	0.175	0.175	0.175	0.175
10	0.175	0.175	0.175	0.176	0.176	0.177	0.176	0.176	0.176	0.176
20	0.182	0.181	0.182	0.182	0.181	0.180	0.178	0.177	0.175	0.175
30	0.182	0.183	0.182	0.181	0.179	0.178	0.176	0.175	0.174	0.174
40	0.180	0.181	0.179	0.178	0.177	0.175	0.173	0.171	0.170	0.170
50	0.183	0.183	0.183	0.181	0.179	0.177	0.175	0.173	0.172	0.172
60	0.181	0.181	0.180	0.179	0.178	0.176	0.176	0.175	0.175	0.174
70	0.182	0.181	0.181	0.180	0.179	0.177	0.175	0.174	0.172	0.172
80	0.178	0.178	0.178	0.177	0.176	0.174	0.172	0.172	0.170	0.171
90	0.178	0.178	0.177	0.176	0.176	0.174	0.173	0.172	0.171	0.170
100	0.179	0.179	0.178	0.178	0.177	0.176	0.175	0.173	0.171	0.171
110	0.181	0.181	0.180	0.180	0.179	0.178	0.177	0.176	0.175	0.175
120	0.185	0.184	0.184	0.183	0.183	0.182	0.180	0.180	0.179	0.179
130	0.187	0.187	0.187	0.187	0.186	0.185	0.184	0.183	0.182	0.181
140	0.192	0.192	0.191	0.190	0.190	0.189	0.189	0.189	0.187	0.186
150	0.194	0.194	0.194	0.193	0.193	0.192	0.192	0.190	0.190	0.189
160	0.198	0.198	0.198	0.198	0.198	0.198	0.198	0.198	0.198	0.198
170	0.200	0.200	0.200	0.200	0.200	0.200	0.200	0.200	0.200	0.200
180	0.201	0.201	0.201	0.201	0.201	0.201	0.201	0.201	0.201	0.201

LITERATURE CITED

Cox, C., and W. Munk
1955. Some problems in optical oceanography. J. Mar. Res., vol. 14, pp. 63–78.
Duntley, S. Q.
1952. The visibility of submerged objects. Visibility Laboratory Final Report, 74 pp.
Duntley, S. Q., R. J. Uhl, R. W. Austin, A. R. Boileau, and J. E. Tyler
1955. An underwater photometer. J. Opt. Soc. Am., vol. 45, p. 904(A).
Gershun, A.
1939. The light field. J. Math. and Physics, vol. 18, pp. 51–151.
Jerlov, N. G.
1951. Optical studies of ocean waters. Reports of the Swedish Deep-Sea Expedition, 1947–48. Vol. 3, Physics and Chem., no. 1, pp. 1–59, Göteborg, Hans Pettersson, editor.
Johnson, N. G., and G. Liljequist
1938. On the angular distribution of submarine daylight and the total submarine illumination. Svenska Hydrografisk Biologiska Kommissionens Skrifter. Ny. Serie Hydrographi, vol. 14, pp. 3–15.
Pettersson, Hans
1938. Measurements of the angular distribution of submarine light. Rapport et Procès-verbaux des Réunions du Conseil Permanent International Pour l'Exploration de la Mer, vol. 108, pt. 2, Light Measurements, pp. 9–12.
Poole, H. N.
1945. The angular distribution of submarine daylight in deep water. Sci. Proc. of Royal Dublin Soc., vol. 24, no. 4, pp. 29–42.
Preisendorfer, R. W.
1957*a*. Mathematical foundation for radiative transfer. J. Math. and Mech., vol. 6, pp. 685–730.
1957*b*. Model for radiance distribution in natural hydrosols. J. Opt. Soc. Am., vol. 47, pp. 1046(A).
1957*c*. Divergence of the light field in optical media. J. Opt. Soc. Am., vol. 47, pp. 1055(A).
1958*a*. On the existence of characteristic diffuse light in natural water. Scripps Inst. Ocean. Ref. no. 58–59.
1958*b*. Some practical consequences of the asymptotic radiance hypothesis. Scripps Inst. Ocean. Ref. no. 58–60.
Takenouti, Y.
1940. Angular distribution of submarine solar radiations and the effect of altitude of the sun upon the extinction coefficient. Bull. Japanese Soc. of Sci. Fisheries, vol. 8, pp. 213–219.
Tyler, J. E.
1955. Measurement of light in the sea. J. Opt. Soc. Am., vol. 45, pp. 904(A)
Whitney, L. V.
1941*a*. The angular distribution of characteristic diffuse light in natural waters. J. Mar. Res., vol. 4, pp. 122–131.
1941*b*. A general law of diminutions of light intensity in natural waters and the percent of diffuse light at different depths. J. Opt. Soc. Am., vol. 31, pp. 714–722.

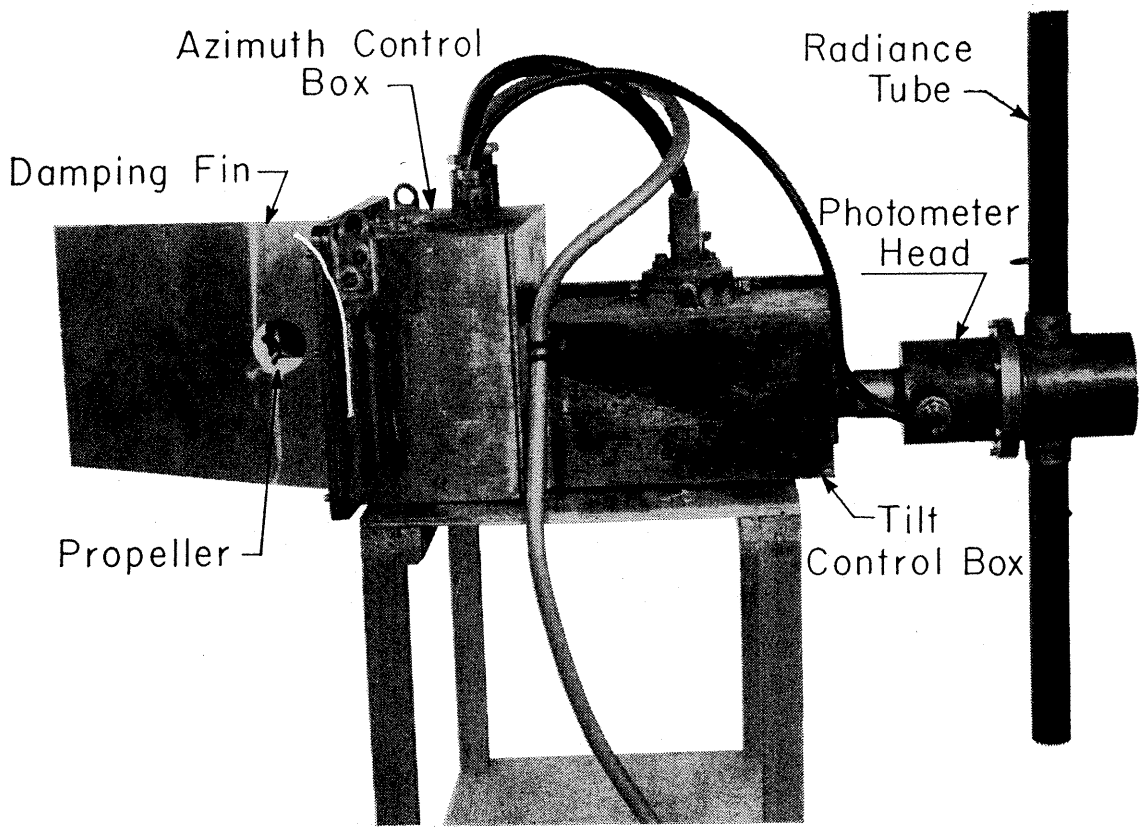

Underwater photometer measuring head and positioning mechanisms.

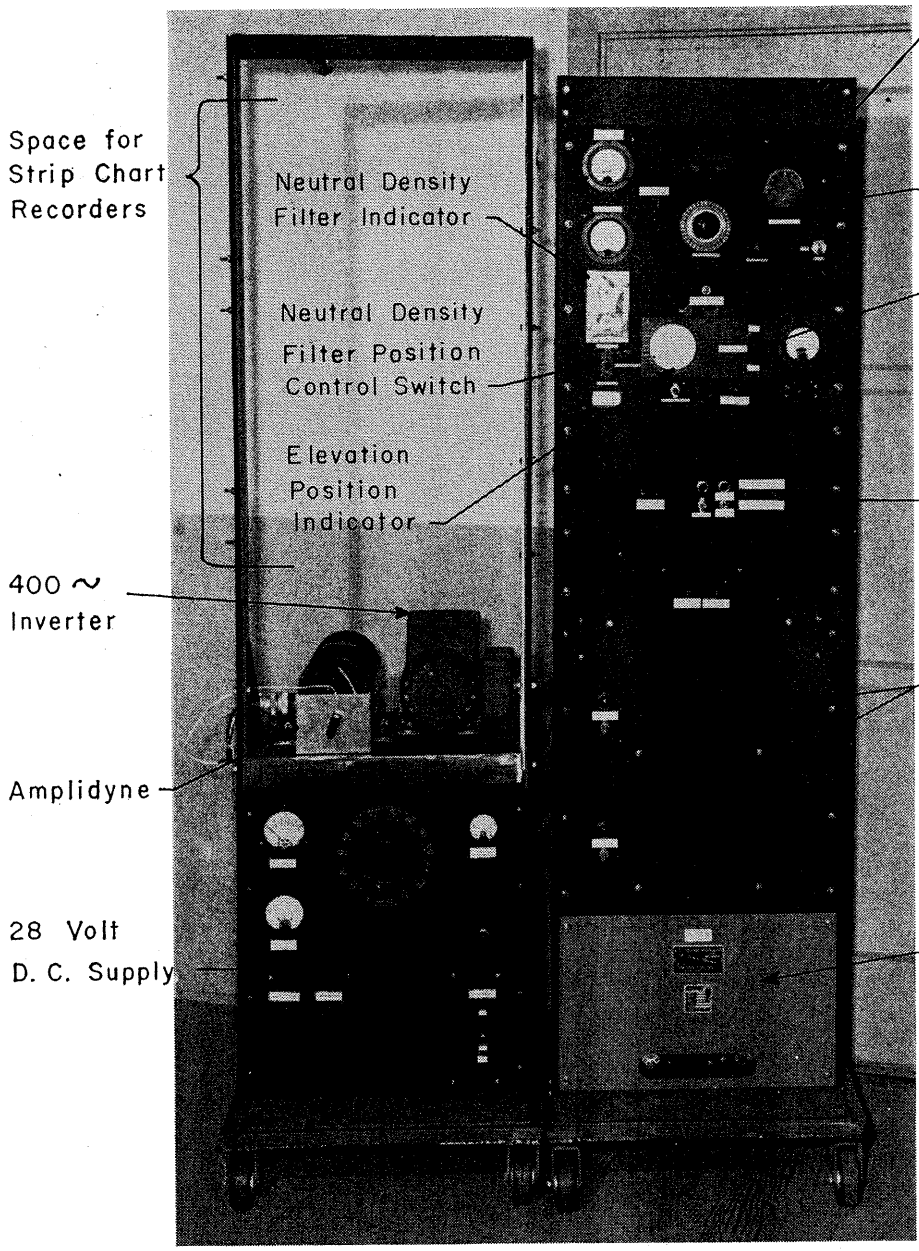

Underwater photometer control panel and power supply.

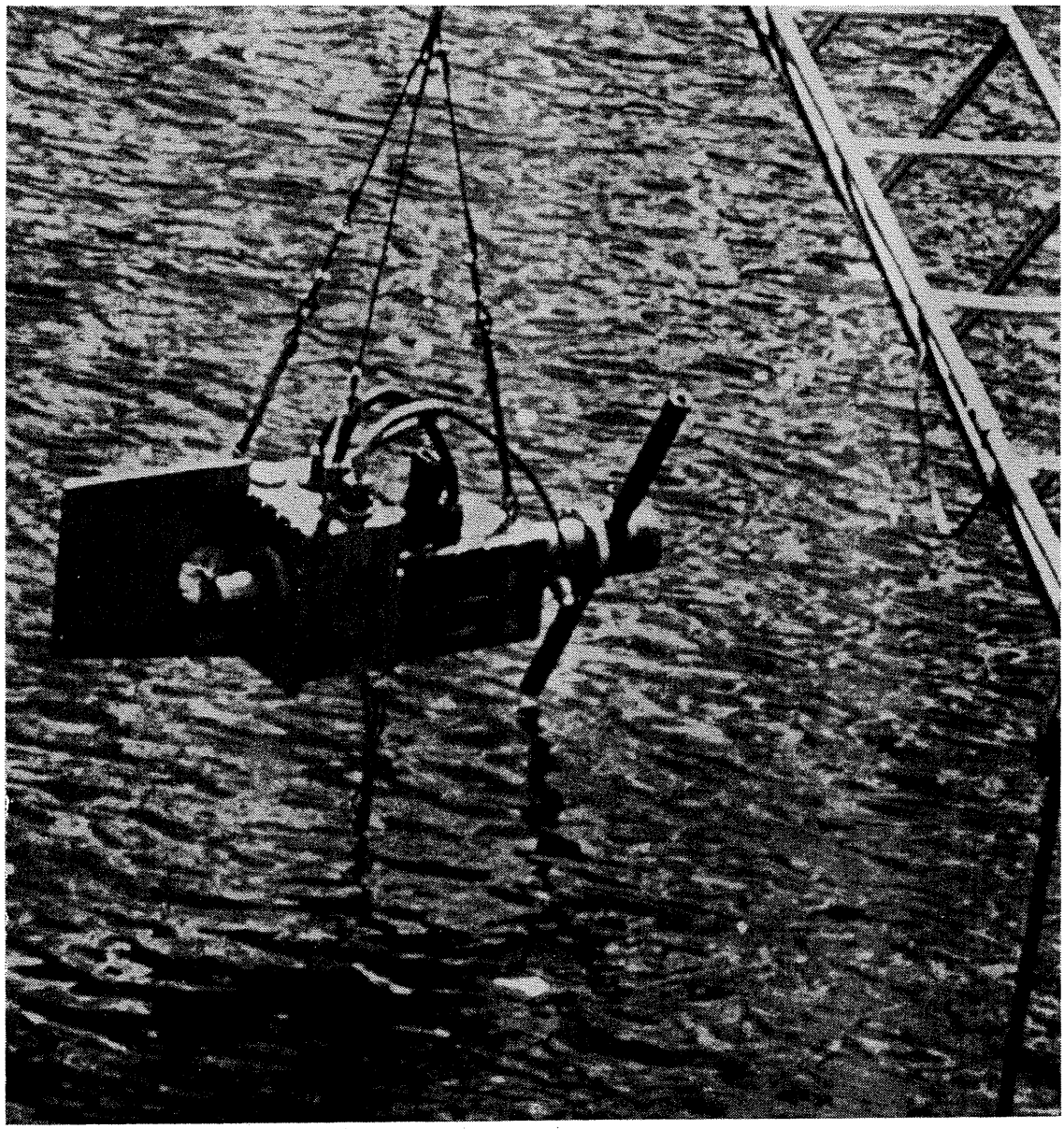

The underwater photometer mounted and ready for lowering into Lake Pend Oreille, Idaho. The measuring head with its Gershun tubes is on the right and the propeller and damping fin are on the left.

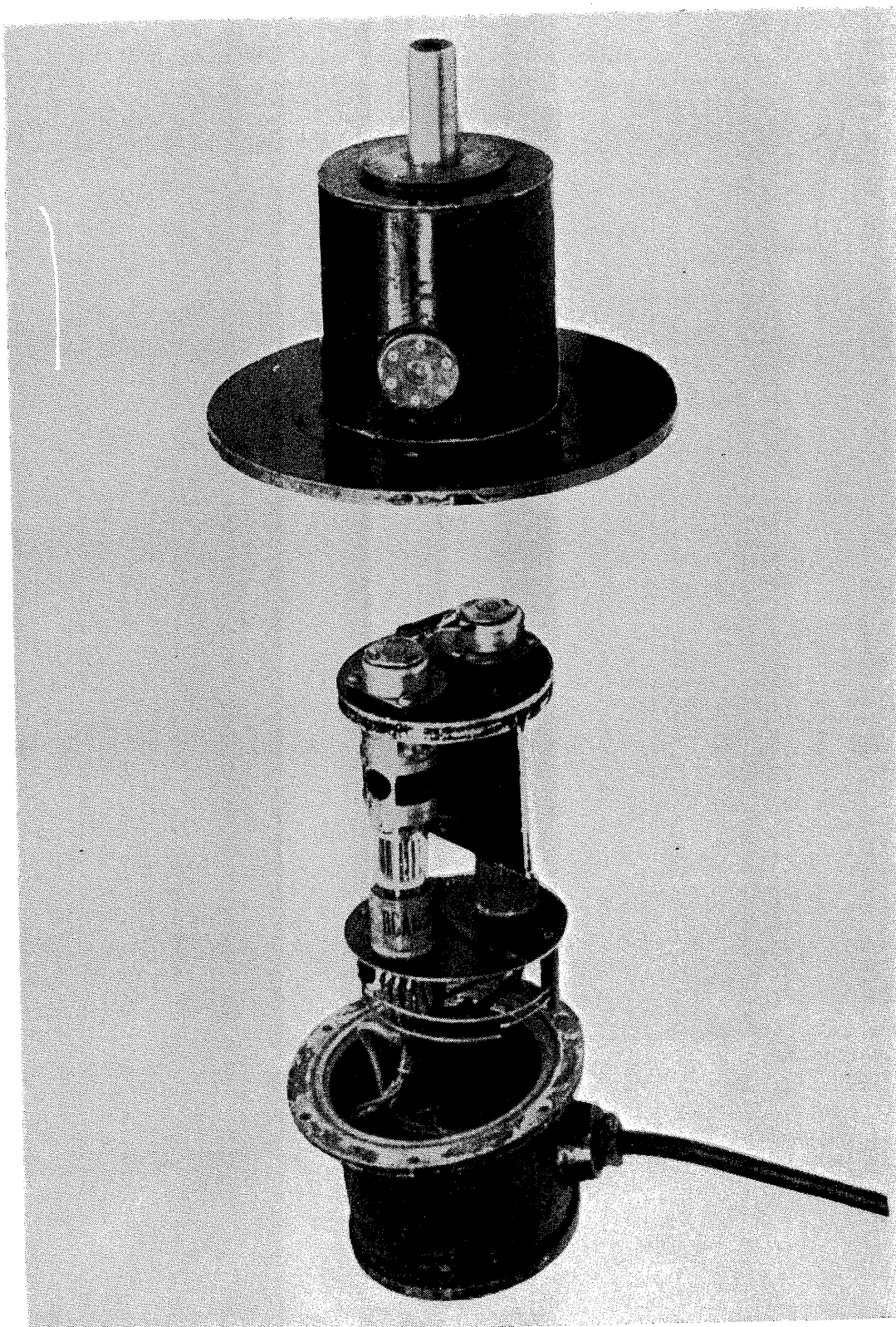

Disassembled view of the measuring head of the underwater photometer. The two mu
phototubes with the cylinders containing neutral density steps can be seen in the central as
The Gershun tubes (not shown) are mounted over the windows, one of which is shown
housing at the top.

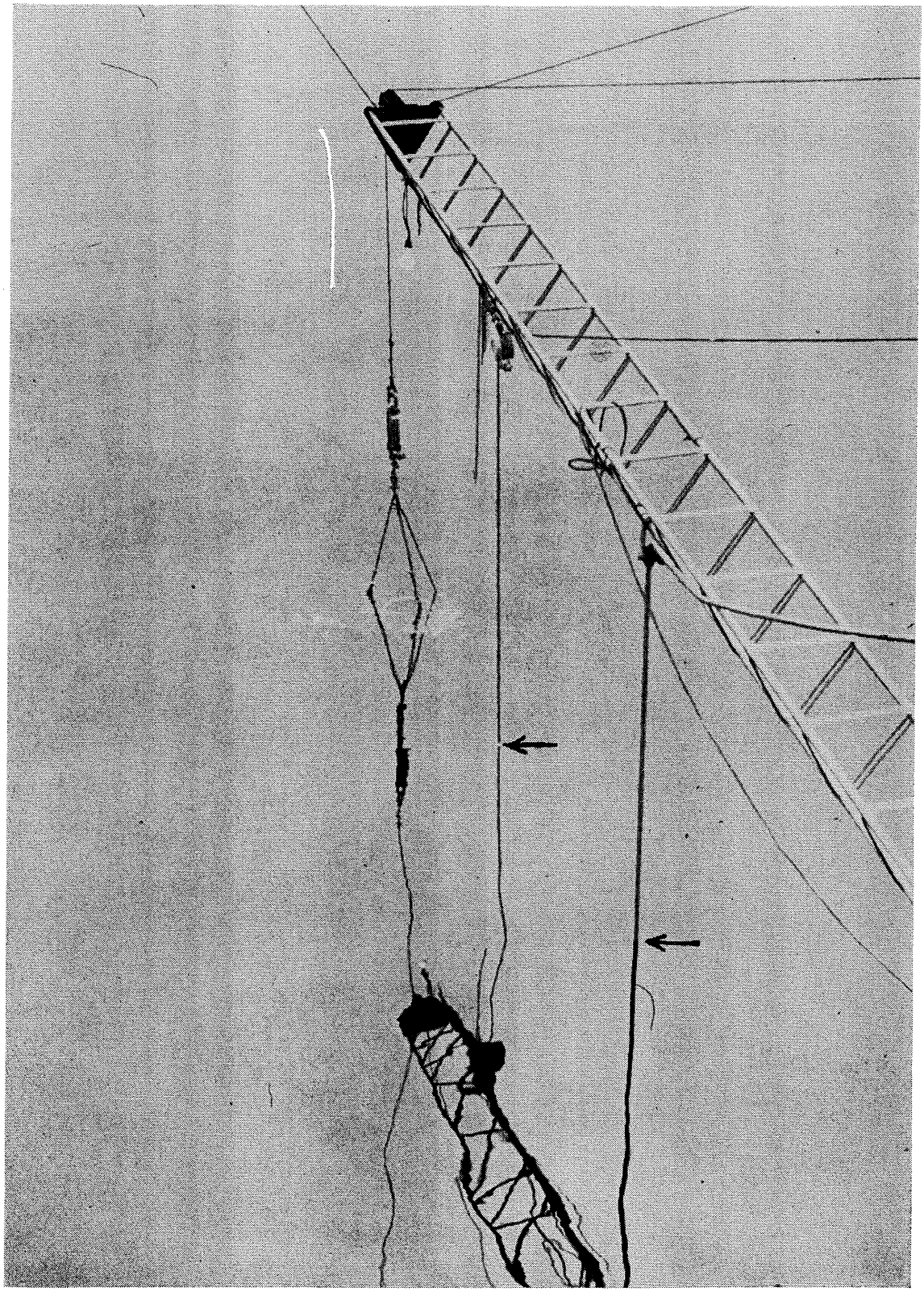

Optical state of the lake surface on 28 April. Arrows indicate points where wires pass through air-water interface.